

LICENTIATE THESIS

Study of particle-current-electrocrystallization interactions in electroplating of Ni/SiC coatings

Santiago Pinate



JÖNKÖPING UNIVERSITY

School of Engineering

Department of Materials and Manufacturing

SCHOOL OF ENGINEERING, JÖNKÖPING UNIVERSITY

Jönköping, Sweden 2019

Licentiate Thesis in Materials and Manufacturing

Study of particle-current-electrocrystallization interactions in electroplating of Ni/SiC coatings

Santiago Pinate

Department of Materials and Manufacturing
School of Engineering, Jönköping University
SE-551 11 Jönköping, Sweden
santiago.pinate@ju.se

© 2019 Santiago Pinate

Research Series from the School of Engineering, Jönköping University
Department of Materials and Manufacturing
Dissertation Series No. 039, 2019
ISBN: 978-91-87289-41-5

Published and Distributed by
School of Engineering, Jönköping University
P.O. Box 1026
SE-551 11 Jönköping, Sweden
www.ju.se

Printed in Sweden by
BrandFactory AB, 2019

ABSTRACT

Composite coatings have great potential due to the possibility to combine properties of two different materials in one coating. This way, new surface properties can be tailored and applied to any material's surface. Among different manufacturing routes, electrodeposition has the biggest potential in creating composite metal matrix coatings, especially nanocomposites. Nevertheless, there is a knowledge gap between the deposition of composite coatings in laboratory conditions, described in the literature, and those that are now in place on an industrial level. While microcomposites have been industrialised for about ten years, the production of Ni/SiC nanocomposite coatings by electroplating is still far from an industrial manufacturing floor. This is due to the lack of understanding of the mechanisms of nanoparticles codeposition leading to scattering results.

The production of nanocomposite coatings is much more sensitive to the process parameters compared to microcomposite. The correlation between parameters and their influence on the codeposition are still not fully identified and understood. The codeposition models proposed in the literature are only valid in specific conditions, but composite depositions behave differently, or even opposite if some of the variables are modified.

The main objective of this work is to identify the particle-current-electrocrystallization interactions in the production of Ni/SiC nanocomposites. A series of experiments are designed to isolate single variables and identify the controlling parameters of these interactions and their impact on the final properties.

In this thesis, the effect of current density, type of current and particles size are identified as primary variables controlling the metal crystallisation and coatings properties.

Among many parameters, a specific current waveform in pulse reverse mode proved to increase the codeposition rate effectively, doubling the content of nanoparticles compared to other techniques. Ultrasound assistance is also considered as stirring method when particles are suspended in the deposition bath to increase their stability and dispersion. The effect of Ultrasound on the particles codeposition and metal crystallisation is studied and compared to silent condition.

Moreover, a surface treatment for the particle has been proven successful in making any particle to behave similarly in the Ni deposition bath. Furthermore, the codeposition rate doubled or tripled compared to untreated ones thanks to this treatment. Both ultrasonic agitation and surface treatment reduce the formation of aggregates, improving the particle dispersion and metal microstructure thus increasing the final hardness.

The work proved the synergistic effect between particle and metal microstructure which affected the final properties of the coating. Therefore, when tailoring the composite coating to improve hardness, it is not only the amount of the particles that should be considered but also their influence on the electrocrystallisation process.

Keywords: Composite coatings; Nanoparticles; Electrocrystallisation; Microstructure; Surface treatment; Pulse plating; Ultrasound agitation.

SAMMANFATTNING

Kompositbeläggning har stort potential tack vare möjligheten att kombinera två material i samma ytskikt. På detta sätt kan nya ytegenskaper skräddarsys och appliceras på ett materials yta. Elektrodeposition är den tillverkningsmetod som har störst potential att uppnå kompositbeläggningar, i synnerhet nanokompositer. Ett kunskapsgap existerar mellan elektrodeposition under laboratorieförhållanden, som beskrivet i vetenskaplig litteratur, och hur processen går till i industriell miljö. Medan industriell tillämpning av mikrokompositer pågått ungefär tio år, så har produktion av Ni/SiC nanokompositbeläggningar fortfarande inte nått fabriksgolvet. Detta är en konsekvens av bristande förståelse kring mekanismer för samdeposition av nanopartiklar som leder till varierande resultat.

Produktion av nanokompositbeläggningar är mycket mer känslig för processparametrar jämfört med mikrokompositer. Korrelationer mellan parametrar och dess inverkan på samdeposition är fortfarande inte fullt identifierade och förstådda. Modeller för samdeposition som föreslås i vetenskaplig litteratur är endast giltiga under särskilda förhållanden. Kompositdeposition kan uppvisa avvikande eller till och med motsatt beteende om variabler förändras.

Huvudmålet med detta arbete är att identifiera interaktioner mellan partikel, ström och elektrokristallisering under tillverkning av Ni/SiC nanokompositer. En serie av experiment är utvecklade för att isolera variabler och identifiera de parametrarna som kontrollerar dessa interaktioner och dess inverkan på ytans egenskaper.

I denna avhandling identifieras strömtäthet, typ av ström, och partiklars storlek som primära variabler som kontrollerar metallkristallisering och beläggnings egenskaper.

Bland många parametrar, visades en specifik vågform på strömmen i omvänd pulsläge öka samdepositionen effektivt, ledande till en fördubbling av andelen nanopartiklar jämfört med andra tekniker. Ultraljud tillämpades som metod för omrörning av depositionsbadet för förbättrad stabilitet och fördelning. Effekten av ultraljud på samdepositionen av metallkristallisering studeras och jämfört med tyst tillstånd.

Dessutom har en ytbehandling för partiklarna visats framgångsrik för att få godtyckliga partiklar att bete sig likt Ni i depositionsbadet. Detta ledde till att samdepositionens takt ökade med en faktor av två till tre jämfört med obehandlade partiklar. Både ultraljud och ytbehandling av partiklarna ledde till minskad aggregation vilket förbättrade fördelningen av partiklar och metallstruktur och därigenom ökad hårdhet.

Arbetet bevisar synergieffekten mellan partiklar och metallstruktur vilket påverkar beläggnings slutliga egenskaper. Vid utveckling av nya ytbeläggningar ska därför inte bara mängden partiklar beaktas utan även dess interaktion med elektrokristalliseringsprocessen.

Nyckelord: Kompositbeläggningar; Nanopartiklar; Elektrokristallisering; Mikrostruktur; Ytbehandling; Pulsplätning; Ultraljudsomrörning

ACKNOWLEDGEMENTS

I would like to express my sincere gratitude to:

The KK-foundation for the financial support of the project FunDisCo (project reference number 20310117).

The industrial partners in the FunDisCo consortium Husqvarna, Swedev, LPTech, Candor Sweden, who made possible this research project.

My main supervisor, Assoc. Prof. Caterina Zanella for the continuous patient, effort, support and criticism, and care in developing my research skills.

My supervisor Prof. Leisner for his valuable comments and suggestions, meaningful scientific talks and assistance.

COST Action MP1407 for providing the funds and support the author's Short term Scientific Mission hosted in Technische Universität Ilmenau, Germany.

e-MINDS training school for financing my participation. Thank you to all committee members.

Technische Universität Ilmenau, and especially Prof. Andreas Bund and Dr. Adriana Ispas for hosting my visit and assistance in the ζ -potential characterisation.

The contribution of Assoc. Prof. Fredrik Eriksson with the XRD measurements.

All my colleagues and friends at the Department of Material and Manufacturing. I am especially thankful for the support provided by Assist. Prof. Ehsan Ghassemali and Jacob Steggo with some of the analysis and experimental work.

My Parents and Siblings. I am forever grateful for your support and endless love.

My adoptive family in Sweden, Jerri, Anna and Lisa.

My fiancée Sofia. Your love and support make me feel at home.

Santiago Piñate Horrillo

Jönköping 2019

SUPPLEMENTS

The following supplements constitute the basis of this thesis:

Supplement I

S. Pinate, F. Eriksson, P. Leisner, C. Zanella; Effects of particles codeposition and ultrasound agitation on the electrocrystallisation of Ni nanocomposites.

Manuscript. Submitted for journal publication.

S. Pinate was the main author. S. Pinate conceived, designed, performed and analysed the experimental work. The author also co-wrote and revised the manuscript. F. Eriksson performed, analysed and wrote the XRD analysis. The author also revised the manuscript. P. Leisner contributed with advice regarding the work, analysed the results, and revised the manuscript. C. Zanella conceived, designed, and analysed the experimental work. The author also co-wrote and revised the manuscript.

Supplement II

S. Pinate, A. Ispas, P. Leisner, A. Bund, C. Zanella; Electrocodeposition of Ni composites and surface modification of SiC nanoparticles.

Manuscript.

S. Pinate was the main author. S. Pinate conceived, designed, performed and analysed the experimental work. The author also co-wrote and revised the manuscript. A. Ispas advised in the design and performed part of the ζ -potential measurements. A. Bund advised in the ζ -potential analysis. P. Leisner designed and analysed the experimental work. The author also co-wrote and revised the manuscript. C. Zanella conceived, designed, and analysed the experimental work. The author also revised the manuscript.

Supplement III

S. Pinate, P. Leisner, C. Zanella; Codeposition of nano-SiC particles by pulse-reverse electroplating.

Manuscript.

S. Pinate was the main author. S. Pinate conceived, designed, performed and analysed the experimental work. The author also co-wrote and revised the manuscript. P. Leisner designed and analysed the experimental work. The author also co-wrote and revised the manuscript. C. Zanella conceived, designed, and analysed the experimental work. The author also revised the manuscript.

TABLE OF CONTENTS

CHAPTER I INTRODUCTION	1
1.1 BACKGROUND	1
1.2 NICKEL ELECTROPLATING.....	2
1.2.1 Electrocrystallisation	3
1.2.2 Electrodeposition setup parameters and their influence on the process	4
1.3 COMPOSITE ELECTROPLATING	5
1.3.1 Particle-Chemical interaction.....	7
1.3.2 Particle transport.....	8
1.3.3 Electric current.....	9
1.4 STATE OF ART	9
CHAPTER 2 RESEARCH OBJECTIVE.....	11
2.1 PURPOSE AND AIM	11
2.2 RESEARCH QUESTIONS	12
CHAPTER 3 RESEARCH APPROACH	13
3.1 RESEARCH DESIGN AND METHODOLOGY	13
3.1.1 Research strategy.....	13
3.1.2 Research ethics and quality assurance	14
3.2 MATERIAL AND EXPERIMENTAL PROCEDURE	14
3.2.1 Nickel electrolyte.....	14
3.2.2 SiC Nanoparticles	15
3.2.3 Electric current.....	15
3.3 CHARACTERISATION AND TESTING	16
3.3.1 Sample preparation.....	16
3.3.2 Characterisation of particles in suspension	16
3.3.3 Imaging techniques	17
3.3.4 Non-Imaging techniques.....	17
CHAPTER 4 SUMMARY OF RESULTS AND DISCUSSION	21
4.1 CHARACTERIZATION OF THE SIC PARTICLE- NI ELECTROLYTE INTERACTION	21
4.2 ELECTROCODEPOSITION AND SIC PARTICLE	25
4.3 PULSE ELECTRODEPOSITION OF COMPOSITE COATINGS	27
4.4 CODEPOSITION OF SIC AND ITS INFLUENCE IN NI ELECTROCRYSTALLISATION	28
CHAPTER 5 CONCLUSIONS	35
CHAPTER 6 FUTURE WORK.....	37
REFERENCES.....	39
APPENDED PAPERS	45

INTRODUCTION

CHAPTER INTRODUCTION

The purpose of this chapter is to introduce the reader to some important definitions and concepts related to the electrodeposition of Ni/SiC nanocomposites that will be used in the following chapters. The chapter starts with a small introduction on electroplating of nickel and continues with a short description of the influence of the process parameters on the SiC nanoparticles.

1.1 BACKGROUND

The surfaces of all components or devices are exposed to different types of loads. Moving parts are in constant friction or must withstand impact-related deformation, or when exposed to ambient, endure possible corrosive environments. Coatings have been developed with many different goals in mind. Among them to serve as surface protection for the bulk material from all the combination of the situations mentioned above to improve both component's performance and lifetime [1].

Hard chromium coatings have been used for protection from wear and corrosion for decades. We can recognise these coatings in car components, tools and cutting devices, and in urban mobiliary due to its outstanding properties of resisting wear and corrosion in challenging conditions [2]. However, the European Chemicals Agency (ECHA) has subscribed in REACH ("Registration, Evaluation, Authorisation and Restriction of Chemicals") the restriction of hexavalent chromium [3], key ingredient in the electrodeposition of chromium coatings because of the environmental hazard and its carcinogenic threat on humans. This has forced the European companies to adapt and search different alternatives to substitute chromium coatings with materials that provide similar properties and performance following the new regulations.

It has been under consideration for a long time the use of composite coatings as a solution. The benefit of using composite materials is that it is combined two materials forming a matrix and a second phase [1]. It has been placed a special interest in electrodeposited composite coatings. A metallic matrix is codeposited with ceramic particles as a reinforcer, which enhances the wear resistance without sacrificing the corrosion protection of the metal matrix [2]. The industry directed the development of these systems toward those materials and fabrication methods that were mature and already in place, being the electrodeposition of Ni/SiC microcomposites one of them [4,5].

Electroplating produces the composite coatings by an electric potential that induces the metal deposition by its reduction on the surface to be coated. The growing metal captures the reinforcer that is in suspension in the electrolyte [6]. Therefore, by controlling the parameters of the process: electrolyte, particles and electric current,

the electrocodeposition is under control [7]. Nevertheless, these micro-sized particles would not be welcome in some of the application where chromium coatings are nowadays in place, e.g. thin coatings, or where large particle could damage the sliding surface behaving like a third body. So, nano-sized particles are more promising, and during the last decades, different scientific studies have reported how these particles are outperforming the micro-sized ones [8–12]. However, the interaction with the process parameters is not fully understood, leading to uncontrolled processes with no industrial application yet. Thus, a great emphasis has been placed in the study of the influence of the process parameters in the behaviour of the nanoparticles.

1.2 NICKEL ELECTROPLATING

Electrodeposition is defined [6] as the process where a metallic film is formed onto a surface through the electrochemical reduction of metal ions from an electrolyte. This technic can be used to electroplate nickel, as represented in Figure 1, where the electrolyte contains nickel salts and soluble nickel anodes are generally used to replenish the Ni ions.

The electroplating of nickel is known for its sensitivity to the electrolyte pH [6]. Nickel's Pourbaix diagram (Figure 2) illustrates how at lower pH (pH < 3) the hydrogen reduction becomes more intense, resulting in a decrease in current efficiency (CE) and possible hydrogenation of the nickel deposit. On the contrary, at higher pH (pH > 5) nickel hydroxides begin to precipitate and could be incorporated into the deposit. Because of this sensitivity to the changes in pH, nickel electrolytes contain buffer agents. These buffers will help to control the increase in pH in the vicinity of the cathode due to the hydrogen evolution which could cause an increase of up to 2 pH units higher than in the bulk electrolyte [6].

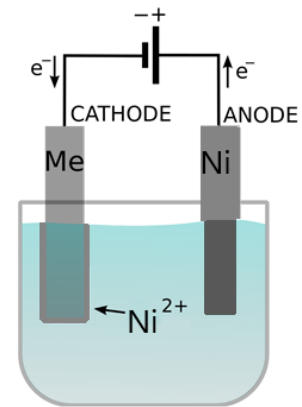


Figure 1: Electroplating of nickel.

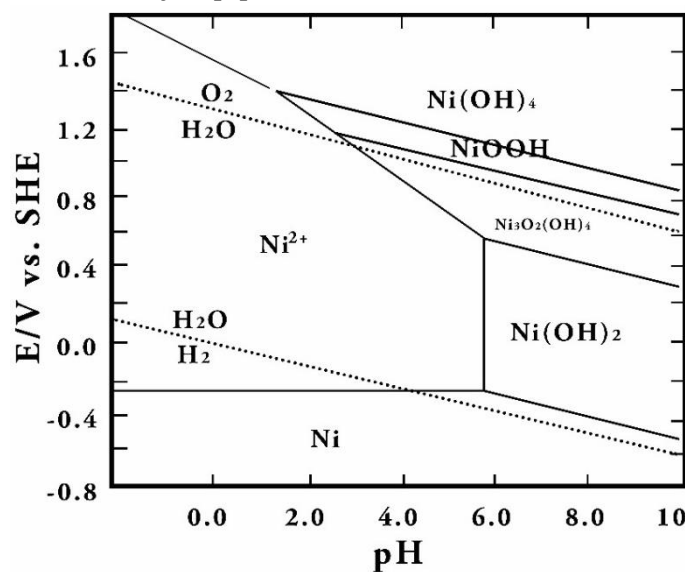


Figure 2: Nickel's Pourbaix diagram, adapted from Lennon et al. [13]

1.2.1 Electrocrystallisation

During electroplating, a transfer of electrons occurs through the electrodes. The metal ions travel towards the cathode and then are reduced into their metallic form. This process can be divided into sequential steps [6] (Figure 3). Firstly, the species to be reduced are carried by mass transfer to the cathode (Figure 3 – step 1). This happens by diffusion, convection and electromigration from the electrolyte's bulk. Second, charge transfer occurs on the cathode, and the partially reduced metal atoms are adsorbed at the surface becoming adatoms (Figure 3 – step 2). Last, loosely bound adatoms will diffuse across the electrode surface to active growth sites, where they are incorporated into the crystal lattice at the kink sites or an atomic step [13] (Figure 3 – step 3).

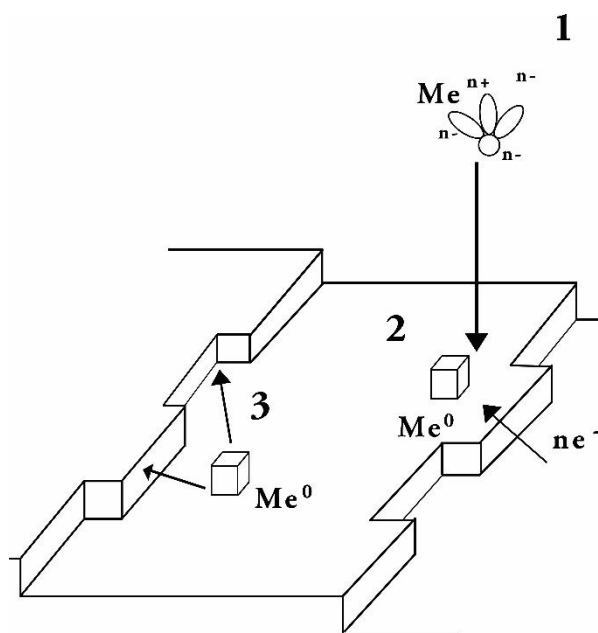
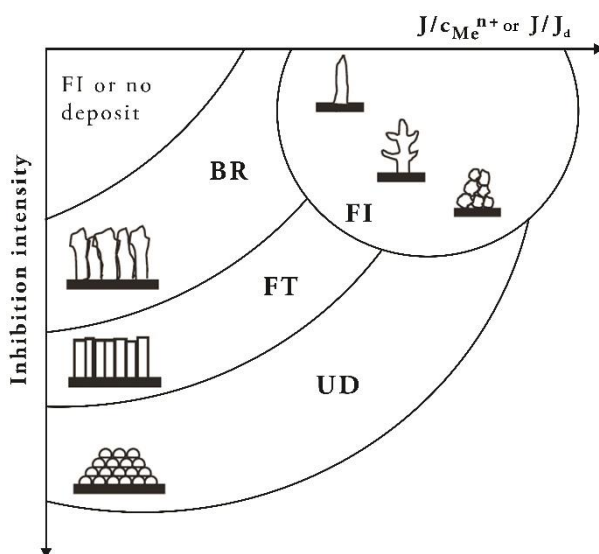


Figure 3: Schematic representation adapted from Gamburg et al. [6] the sequential steps of an electrocrystallization process. (1) Mass transfer of the metal ion, (2) Charge transfer and partial adsorption of the adion, (3) Diffusion of adion to an active growth site.

The kinetics of the electrocrystallisation are described by the Butler–Volmer equation [6,13], given an applied overpotential, it determines the charge transfer reaction rate, hence the metal deposition rate. The growth mode of the electrodeposited metal varies depending on the inhibition provided by the additives in the electrolyte and the relative current density, which would lead to different atom arrangements in the crystal lattice [13,14]. In nickel electrodeposition, this inhibition not only can be caused by additives but also by electroplating byproducts. Hydrogen adsorption (H_{ads}), gaseous H_2 , and $Ni(OH)_2$ will act as inhibitors and promote different growth modes. Depending on the type of growth different microstructures can be formed. Winand [15] classified the different microstructures, depicted in Figure 4, which are the most commonly encountered.



Winand [15] classified the different microstructures, depicted in Figure 4, which are the most commonly encountered.

Figure 4: Diagram adapted from Winand [15], showing different types of microstructures as function of the current density and metal ion concentration ($J/C_{Me^{z+}}$) or the diffusion limiting current (J/J_d), and the inhibition intensity.

Where:

- FI: Field oriented isolated crystals type;
- BR: Basis oriented reproduction type;
- FT: Field oriented texture type;
- UD: Unoriented dispersion type.

In electrodeposition with uninhibited or low inhibition growth, the adatoms discharge and attach across the whole surface, forming isolated nuclei which would grow vertically [13]. In nickel, this is known as normal or non-inhibited growth, and it is dominated by the [100] texture [14]. In some cases, additives or electroplating byproducts would be preferentially adsorbed at the active growth sites, i.e. at kinks and atom steps; forcing the metal ion to discharge in the atom plane, forming a new layer where a newly formed nuclei would grow. This moderate inhibition is seen in Ni when some of the hydrogen is atomically adsorbed stabilising the <110> growth mode, or the <210> direction is favoured by gaseous hydrogen. Finally, when strongly inhibited, a layer by layer growth dominates the deposition. A known strong inhibitor in Ni electrodeposition is nickel hydroxide which leads to deposits with a <111> preferential growth. In general, deposits that grow non-inhibited are dominated by a single growth mode [100], while those that grow under inhibiting species are randomly orientated with no preferential growth [14].

1.2.2 Electrodeposition setup parameters and their influence on the process

The electrodeposition setup requires the following components (Figure 1): (i) the electrode where the metal reduction ensues, i.e. the surface to be coated, referred as cathode, (ii) an anode, where the oxidation takes place, (iii) an electrolyte which works as the medium transporting the current between electrodes, and (iv) an external power supply. All these components can be adjusted as variable parameters, especially the last two. Multiple parameters constitute the electrolyte: composition, pH, temperature, and agitation could be modified to influence the characteristics of the deposit [6,16–18]. Likewise, the current or voltage supplied by the external power supplier could be tuned to tailor at will the deposits' properties by changing the current intensity or type [15,19]. It is common that one or more of these parameters are fixed variables to analyse the synergetic relationship between the remaining.

1.2.2.1 Electrolytic bath

Each parameter of the bath plays an active role in the deposition [6]. The electrolyte composition is mainly composed of Ni salts that are dissolved in water. The most two common nickel bath formulation is the Watt's bath [20], based on the use of nickel sulphate, and the sulfamate bath, based on the use of nickel sulfamate as nickel source. In both cases, nickel chloride is often added to increase the solution's conductivity while the chloride ions help to dissolve the anode by avoiding passivation. High levels of chloride concentration can affect the deposit ductility and the coating's internal stresses.

Additionally, boric acid is also added as a buffering agent to limit the changes in pH at the cathode during electroplating. These formulations can also include additives which provide a uniform fine grain structure of the nickel plating [21], called grain-refiners. Other additives that are commonly added are the wetting agents. These additives are commonly referred to as surfactants, and they facilitate the release of the clinging hydrogen bubbles formed at the electrode during electrodeposition; helping to avoid porosity [22]. Other additives are levellers which help to fill pre-existing voids in the cathode's surface and brighteners for a bright surface finish.

The temperature can be increased to improve the solubility of the species and the conductivity of the electrolyte [6]. Furthermore, as previously mentioned pH value also influences the side reactions such as hydrogen evolution and unwanted nickel hydroxides (Figure 2). The current efficiency of the process is also influenced by H^+ reduction. To enhance the ionic transport from the bulk to the electrode it is preferred an electrolyte's stirring. There are different types: mechanical and ultrasound (US). However, the intensity of the stirring could hinder the adhesion of the coating.

1.2.2.2 Electric current

An electric potential is used to form an electrolytic cell which simultaneously reduces and oxidises the metal forming the metallic coating. Depending on the duration of the time in which this potential difference is applied, the current is directly responsible for the amount of deposited metal. The relationship between the current and metal's mass is described as Faraday's law [6]:

$$m = QM/nF$$

Where m is the mass of the deposited metal, Q is the net charge applied to the cell, M is the atomic weight of the metal, n the number of electrons to reduce the metal ion, and F is the Faraday constant. Thus, the imposed electric potential provides control over the electrocrystallisation and the current over the deposition rate of the metal. An important factor is also the current form. Direct current (DC) is the continuous flow of cathodic current, Pulse current (PC) is the alternation of cathodic current and no current (off), and Pulse-reverse current (PRC) is the alternation of cathodic and anodic current between the electrodes. It is possible to control the deposits' coating microstructure by regulating the current density, pulse duty cycle and frequency [23]. Pulse current waveform could favour the initiation of grain nuclei by using high current densities and increase the number of grains per unit area. This results in finer grained structures with better properties than conventionally plated coatings, due to the increased hardness by the Hall-Petch strengthening.

1.3 COMPOSITE ELECTROPLATING

The electrodeposition of nickel coatings containing SiC particles involves three main processes. The physical dispersion of particles in the electrolyte, their transport to the cathode and their entrapment by the growing metal. As discussed previously, the parameters that influence the electrocrystallisation: electrolyte and current will affect the mechanisms of the particles' incorporation. Therefore, the effect of operating parameters on different particles size has been studied in the last decades [24]. It had been proposed different models that described and explained the codeposition mechanisms of these dispersion coatings, Table 1 provides an overview of different models and their main assumptions.

Table 1 Theoretical models of the mechanisms of codeposition in composite materials, adapted from Low et al. [24]

Guglielmi, 1972 [25]	Describes both adsorption of metal ions and their transport by electrophoresis to the cathode. Establishes a relationship between particle quantity and current density. The effect of electrolyte flow was not considered.
Celis et al., 1987 [26]	Use probability concept to predict the number of particles that can be incorporated at a given working condition, current density. Thus, mass transport of particles is proportional to the mass transport of ions to the working electrode.
Fransaer et al., 1992 [27]	Extended Celis's model by using trajectory analysis to describe the particle codeposition. The authors proposed two steps: (i) reduction of metal ions (current density), and (ii) codeposition of the particle (trajectory).
Hwang et al., 1993 [28]	Based on Guglielmi's model. Uses different current densities and particle suspension concentration to identify the particle deposition rate by the reduction of the adsorbed ions on particles. The authors proposed three steps: (i) forced convective of particles to surface, (ii) loose adsorption on the surface, and (iii) incorporation of particles by reduction of adsorbed ions.
Vereecken et al., 2000 [29]	The transport of particles to the surface is control by convective-diffusion and their incorporation by the time stays close to the electrocrystallisation front. The model is only expected to hold for particles smaller than the diffusion layer thickness.
Bercot et al., 2002 [30]	An improvement of Guglielmi's model, which incorporates a corrective factor, a 3rd order polynomial equation as a function of the cathode's angular velocity and volume of particles in suspension.

The shortcoming of these models is their rigidity since they have only been proven valid for certain experimental conditions, and they are not reliable outside these constraints. Moreover, these models only account for microparticles and not nano-sized ones. However, these models engage in the importance and influence of the multiple parameters that compose electroplating; this could be extrapolated to the codeposition of SiC nanoparticle. Figure 5 depicts the possible codeposition steps as described by Celis's Model [26]. Figure 5 step-i, is the adsorption of ions on the surface of the particles. Followed by their transport toward the cathode (step-ii) influenced by the surface adsorption and the operating parameters. Ending with the partial adsorption at the cathode's surface (step-iii) and their entrapment (step-iv) by the metal.

Nowadays there are no models in place that theorises the mechanisms of codeposition for nanoparticles, nor it has been established a relationship between the electrodeposition setup and the particle incorporation rate.

Any new model that intends to explain the mechanisms of the codeposition of nanoparticles can be built upon the proposed ones. However, these new models must consider the synergistic effect between the electrodeposition setup parameters and the particle characteristics (chemistry, dimensions, and concentration). The electrolyte formulation and operating temperature and pH will determine the initial particle-chemical interaction.

1.3.1 Particle-Chemical interaction

Guglielmi's model [25] describes the fundamentals of the adsorption that the particles undergo when added to the electrolyte. While in suspension different ions will be adsorbed on the particle's surface, surrounding the particle in an ionic cloud [31]. Depending on the particles' surface charge, anions or cations would be attracted to its surface. All models based on Guglielmi's agree on the importance of the characteristics of this cloud of ions since its sign determines the attraction or repellency of the particles to the cathode's surface, which is negatively charged.

The ζ -potential determines the potential at the outer Helmholtz layer; thus it can be connected to the surface adsorption and surface charge (Figure 6). The ζ -potential can be influenced by the electrolyte's ionic strength, temperature, or type of ions and their concentration because it changes the type of surface adsorption. Several studies [32–35] were focused on the study of the ζ -potential value and how it was influenced by the electrolyte, to describe the codeposition rate based on its value.

Considering the addition of particles into typical Ni-based electrolyte's formulations, it is expected a surface adsorption of metal ions, sulfates or chlorides, and depending on the pH, H^+ and OH^- [31]. In some cases where additives were used, the surface adsorption of the particle could be modified entirely [22,36] because of the cationic

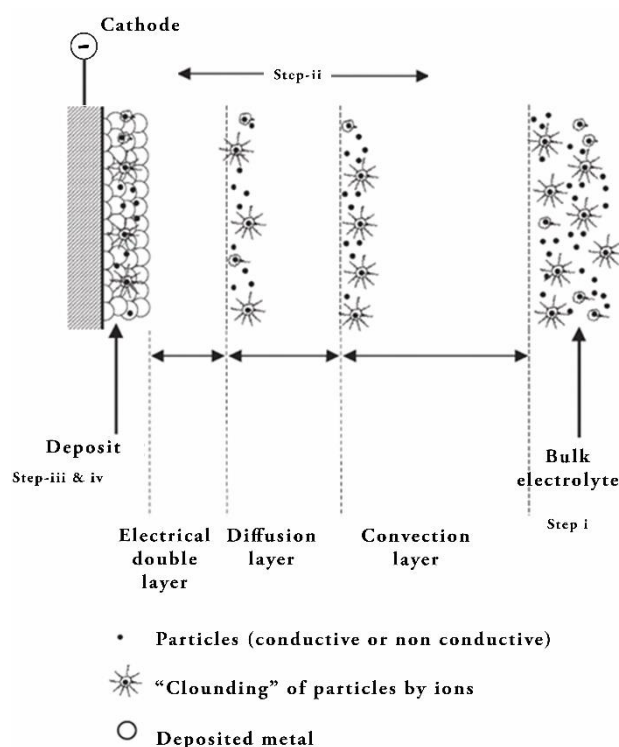


Figure 5: Mechanisms of particle codeposition into a metal deposit, adapted from Celis et al. [26].

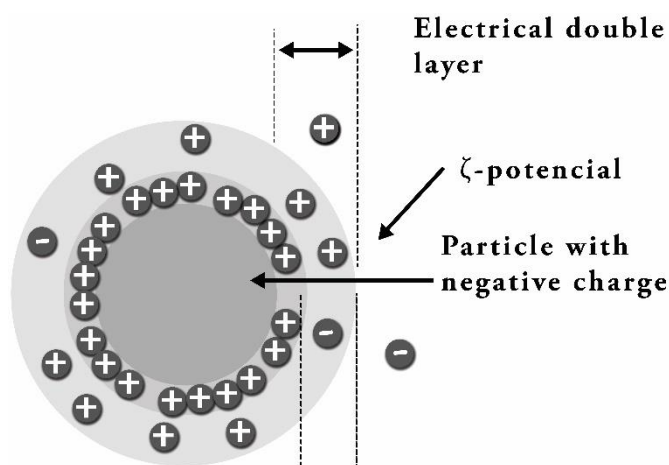


Figure 6: Representation of the ionic cloud adsorbed by a particle with a negative surface charge.

or anionic nature of these additives. So the particle-chemical interaction could greatly vary depending on the characteristic of the particle, the additives and the operating parameters, electrolyte, pH and temperature [22,24,31,36–39]. Depending on the degree of this interaction the particles can flocculate because of the attraction between particles, and sediment if the stability is not high enough to maintain the suspension of the particles. To avoid this, the electrodeposition of composite always requires a continuous agitation, which will affect the particle transport.

1.3.2 Particle transport

Agitation plays two critical roles in the electrodeposition of composites: maintaining the particles in suspension avoiding the flocculation and sedimentation, and interacting with the transport of the particle toward the cathode or the entrapment into the growing metal.

As previously discussed by the codeposition models the mechanisms of transport can be electrophoretic [25], convective-diffusion [26], and by hydrodynamics [27]. Thus, the selection of the agitation mode is critical to particle transport since it can affect any of the three. Electrophoresis refers to the motion of dispersed charged particles under the influence of an electric field. The motion of the particle is dependent on the electric surface charge, or as previously discussed the ζ -potential, and the intensity of the electric field. However, the intensity of the agitation could improve or interfere with this motion [24]. Celis et al. [26] described the convection-diffusion of the particles as the mass transport of a particle surrounded by an ionic cloud toward the cathode, that later diffuses through the double layer accompanied by a reduction of these ions. Any turbulence caused by the agitation would undoubtedly modify the mass transport of ions, thus the kinetics of the particle. Lastly, the hydrodynamics described by Fransear et al. [27] refers to the trajectory of a particle because of the flow of the electrolyte caused by a rotating disc. Hence, any fluid flow velocity given by the agitation mode will vary this trajectory.

The agitation methods used in the electroplating of composites are the agitation by pump, ultrasonic agitation and mechanical stirring. The agitation by pump is only standard on an industrial scale, and no exhaustive research has been done on the topic. The mechanical stirring involves controlling the agitation by RPM. Different studies reported a decrease in the codeposition rate if the stirring speed is low [40,41] because of the particle sedimentation, or if it is too high [42,43] because the particles are removed from the surface before the growing metal entraps them. The ultrasonic (US) agitation is based on an acoustic stream which propagates through the electrolyte by a series of compression and rarefaction cycles [44]. This agitation can be controlled by the ultrasonic power, frequency, sonic source characteristics. When the ultrasonic power is high enough, a cavity or 'bubble' may form [45]. The combination of both the acoustic streaming and cavitation could reduce particles agglomeration, increasing the codeposition rate [46–50]. However, it has been shown [51,52] that a high US power could have the opposite effect, a decrease in the particle content due to a bouncing-back effect when the particles approach the cathode.

1.3.3 Electric current

Electrodeposition of composites can be performed by different galvanostatic techniques, which includes direct current, pulse current and pulse-reverse current. The external power supplier can be set to supply different currents, and specific pulse period and duty cycle. This allows control of the electrocrystallisation of the metal, yet there is not a full understanding of how this affects the codeposition of the particles.

Direct current is the most commonly used to obtain nanocomposites [24]. This technique is based on the incorporation of nanoparticles within the reduction of the metal ion at the cathode. Kollia et al. [19] associated the crystal size to the current density, growing smaller grains with a higher current value. Although, there is a disagreement if high direct current densities are associated with a decrease in the content of particles in the composite coating [9,53] or an increase [54,55]. However, the literature shows an increase in the particle codeposition when pulse current, or pulse-reverse, is used instead [56–61].

Nevertheless, these contradictions could be explained by the fact that these experiments were done in different electrolytes and no direct correlation can be therefore drawn. As earlier described the electrophoretic transport of the particles is a function of the electric field intensity (current density) and the ionic cloud that surrounds the particles (the electrolyte formulation).

In pulse electrodeposition, the current is alternated between two or more cathodic currents or off-time. While pulse-reverse shares the same concept but alternates the cathodic current with an anodic current. This technique allows the control of the different particle transport: (i) The electrophoresis by modifying the current density during the cathodic current. (ii) The convection-diffusion transport by the control of the periods which benefits the replenishment of ions and particles by mass transport. (iii) By increasing the time frame where the particles are close to the cathode during the off-time or anodic pulse, which benefits from the hydrodynamics of the bath. Based on this, Xiong-Skiba et al. [60] and Podlaha et al. [59,62] tailored the current type and density to maximise the codeposition.

1.4 State of Art

A lot of attention has been paid to the characterisation of the particle-chemical interaction by ζ -potential [32,33,36,63–67]. This has brought some light into the comprehension of what type of ions are adsorbed by the SiC nanoparticles, and under what conditions of pH and electrolyte composition. Nevertheless, all these studies were done under the assumption that the particles are pure SiC. Even though the particles possess a high purity, the firsts nanolayers of the surface are very likely oxidised or contain some impurity depending on the very different manufacturing process used to produce them. Moreover very often nanopowder contains some unknown additive or stabilisers to avoid agglomeration. This could change their surface state completely and therefore the ionic adsorption on the surface of the particles when suspended in the electrolytic bath, thus affecting their codeposition.

Although many theoretical models have been proposed, the effect of the particles on the metal electrocrystallization itself has not been considered. This aspect is significant since their inclusion into the metal deposit may cause a reduction of the cathode surface area [39] since the SiC particles are nonconductive. They can also modify the deposit microstructure [38,57,68,69], leading to a change in the properties of the deposit. The effect on the cathode surface area could lead to a decrease in the current efficiency, thus an increase in the hydrogen evolution, a higher change in pH, and the promotion of inhibiting species which alter the normal nickel growth.

Any parameter that promotes a more extended time where the particle sits closer to the cathode promotes a higher codeposition rate. Guglielmi [25] expressed it as the electrophoretic transport, and the particle-cathode attraction. Celis et al. [26], Fransaer et al. [27], and Hwang et al. [28] built upon Guglielmi's model and extended its importance to the mass transport of ions adsorbed on the particles' surface by convection-diffusion. Vereecken et al. [29] stated its fundamental role in the codeposition of submicron particles explicitly. Inspired by this, Podlaha et al. [59,62] and Xiong-Skiba et al. [60] proposed a pulse-reverse waveform to keep the particles close to the cathode. However, due to the extended anodic time, there is a considerable risk of electrode passivation, and this method has not been yet replicated.

RESEARCH OBJECTIVE

CHAPTER INTRODUCTION

This chapter firstly describes the purpose and aim, followed by the research questions.

2.1 PURPOSE AND AIM

The increase in demand for cost-efficient surface treatments that withstand challenging conditions, and that also meet the new environmental regulations encouraged the development of new processes and materials. The restriction on manufacturing chromium coatings put in motion a series of initiatives to effectively substitute this coating with different alternatives, where electrodeposited Ni/SiC composites are one of them. It is because of this industrial need that many efforts are put into the engineering of these nanocomposite coatings, instead of microcomposites. However, none of these attempts has been translated into a functional industrial manufacturing method, because of the lack of control of the process. It is not fully understood how the input parameters of the process are translated into the characteristics of the composite; thus, there is not a total control on the final properties of the coating.

A deeper understanding of the synergistic relationship and the interaction of the process variables will benefit the industrial production of nanocomposite coatings. The research purpose is to complement the different studies done, and available in literature by studying the interactions on the codeposition of the three main factors: particles, current, and electrocrystallization.

A better understanding of the interaction particle-electrolyte will provide a view of the optimal bath parameter setup and how these are related to the particle deposition rate. Furthermore, it is critical to determine the current-particles interaction, to design such a waveform that could consistently produce highly reinforced composite coatings.

The analysis is extended to identify the influence the particles have on the electrocrystallisation of the metal matrix. This will help to develop an awareness of the relationship between microstructure and codeposited particles to the final properties of the deposit.

2.2 RESEARCH QUESTIONS

The previous literature review provided a general theory of nickel and composite electroplating and described the role the different process setups play in the results. From this, it is easy to recognise the importance of obtaining a better understanding of the synergistic effect between parameters, and their influence on the deposits' characteristics and properties.

Therefore, the current research tries to gain a better understanding of the production of Ni/SiC nanocomposite by electrodeposition by answering the following research questions:

1. *When added into the electroplating bath, what is the particle-chemical interaction of the SiC nanoparticles?*
 - a. *Is it possible to control this interaction without modifying the bath setup?*
2. *Is it possible to tailor a current waveform that increases the SiC particles' content?*
3. *What is the role of the presence of SiC particles with different sizes and content during the electrocrystallisation of nickel?*
 - a. *How are the mechanical properties of the deposits affected by the modification of the microstructure?*

RESEARCH APPROACH

CHAPTER INTRODUCTION

This chapter describes the research design used in this thesis. The research methodology is firstly described, followed by a description of the experimental procedures, and the characterisation techniques.

3.1 RESEARCH DESIGN AND METHODOLOGY

3.1.1 Research strategy

The research is based on three research questions, which results are organised in three papers (Figure 7), included in this work as supplements.

Supplement I will include a variation on the agitation mode. In this supplement mechanical and US agitation are compared, producing Ni/SiC composites with different particle size, addressing RQ3. The purpose of supplement II is to study the particle-chemical interactions of SiC particles of different sizes by ζ -potential measurements. The output of Supplement II is a description of how different are the SiC particles, despite an equal theoretical composition; thus, addressing RQ1. This supplement also offers a pretreatment that brings the particles into a common state, having a similar particle-chemical interaction without modifying the original process parameters.

Supplement III focuses on modifying the electric current, varying the type between direct current and pulse-reverse current, and density; adjusting the parameters to selectively entrapped the nanoparticles. This supplement mainly addresses RQ2.

Objective:	Ni/SiC nanocomposites		
	Suppl. I On the electrodeposition of Ni/SiC under US agitation	Suppl. II On the surf. treatment of SiC and the production of nanocomposites	Suppl. III On the electrodeposition of Ni/SiC under Pulse reverse plating
		•	
			•
RQ1: Particle-chemical interaction			
RQ2: Controlling the codeposition by method design			•
RQ3: Influence on the Ni electrocrystallization by SiC particles	•	•	•

Figure 7: Schematic research strategy.

3.1.2 Research ethics and quality assurance

In order to increase the reproducibility of the research, multiple samples are produced and tested under the same conditions. The samples taken randomly from each condition are characterised and compared. To increase reliability, each sample is marked and registered with full preparation details. An experimental journal is updated to track the source of the unforeseen changes in the standard conditions. To ensure the validity of the research, the characterisation of all the samples follows the standardise analysis methodology. This is accompanied, by comparing the results to earlier studies when available. Errors during the experimental works are identified and minimised. The chemicals and salts used in the production of the electrolyte are from the same manufacturer and batch. To assure the same range and quantity of uncontrolled impurities the particles used in the experiments are from the same batch.

3.2 MATERIAL AND EXPERIMENTAL PROCEDURE

In order to benchmark between the results obtained in each supplement, some of the process parameters remained constant in all the experiments and supplements. This is described in the following section.

The electrodeposition is performed in a thermally controlled cell at 45 °C with 500 mL electrolytic bath. The cathode is a low carbon steel plate with a surface of 0.15 dm² and placed in a parallel vertical electrode configuration with a distance between cathode and anode of 7 cm. The anode is a Ni sheet of 99.9% purity. Before plating, the substrates are mechanically ground with SiC grade #1000, cleaned ultrasonically in an alkaline soap and activated by pickling for 8 min in 2.5 M H₂SO₄.

The pH of the plating electrolyte is stabilised at 3.0 before each electrodeposition by adding H₂SO₄ or NaOH. The pH is measured after each deposition and compared to the initial pH. The current efficiency (CE) of the process is obtained by comparing the theoretical deposited mass calculated by Faraday's law to the weight of the deposited mass minus the mass of the particle content. The composite coatings are produced by adding 20 g/L of SiC powder with different average particles sizes. The bath suspension is continuously stirred by a rotating magnet and agitated with ultrasound (US) for 30 minutes before electroplating.

3.2.1 Nickel electrolyte

The electrolyte formulation is based on an additive-free Watt's bath [20], where its composition, pH and temperature remained fix for all the experiments and supplements. The plating bath composition is listed in Table 2.

Table 2: Plating bath formulation based on Watt's bath [20]

Electrolyte composition			
NiSO ₄ ·7H ₂ O	240 g/L	pH	3.0
NiCl ₂ ·6H ₂ O	45 g/L	Temperature	45 °C
H ₃ BO ₃	30 g/L		

3.2.2 SiC Nanoparticles

The composite coatings are produced with SiC particles with different average size.

- Supplement I: SiC powder of nano- (gnm© #SiC-110 β -SiC 50 nm), submicron- (gnm© #SiC-110 β -SiC 500 nm), and micro-size (H.C.Starck© SiC grade UF-05 α -SiC 5 μ m).
- Supplement II: SiC particles of nano- (gnm© #SiC-110 β -SiC 50 nm), nano- (ESK-SiC GmbH. NF25 β -SiC 300 nm), and submicron-size (gnm© #SiC-110 β -SiC 500 nm).
- Supplement III: SiC particles of nano- (gnm© #SiC-110 β -SiC 50 nm).

3.2.2.1 Surface treatment

The particles used in Supplement II included a pre-treatment (described in Suppl. II – Table 2) to compare the results obtained from an as produced state. The surface treatment is done by adding the SiC particles with a load of 20 g/L into 1 litre of distilled water and stirred for 30 minutes. The suspension is then filtered by MUNKTELL© analytical filter paper (Quality 00H, ash content 0.007%), maintaining at least 100 ml of suspension to avoid agglomeration. The suspension is then set to a volume of 1 litre with 20 mL/L nitric acid (65%) and stirred for 15 minutes. The suspension is again filtered and rinsed with distilled water until the pH reaches 6.0. The suspension is continuously stirred (200 rpm).

To avoid the drying and agglomeration of the particles the plating bath, as described in Table 2, is mixed into the SiC-water suspension immediately after the final rinsing. After preparation, the solution is agitated by ultrasound (US) for one hour and the pH adjusted to 3.0.

3.2.3 Electric current

The current type and levels are set for each supplement as follow:

- Supplement I and II: Direct current (DC) at 4 A/dm² for 30 minutes.
- Supplement III: Direct current (DC) at 4 A/dm² and 10 A/dm² for 30 and 12 minutes respectively, and two pulse-reverse current in different waveforms short and long, described in Supplement III – Table 1 and Figure 1. The Long cycle pulse-reverse method used in this supplement is designed to entrap the 50 nm diameter size SiC particles by plating a thickness equivalent to the diameter per cycle and then strip half of the thickness, inspired by the previous work done by Podlaha et al. [59,62] and Xiong-Skiba et al. [60]. Pulse reverse with short pulses (PR-SP) is used as the traditional PR method in order to benchmark the deposits made by pulse reverse with a long cycle. DC densities are set to match the cathodic and the average current densities of PR plating.

3.3 CHARACTERISATION AND TESTING

3.3.1 Sample preparation

The samples are marked according to their production condition and sectioned in a square shape. Only the samples located in the middle of the coating are selected for analyses to avoid areas affected by the edge effect, as pictured in Figure 8a. For the cross-section, the samples are mounted in PolyFast conductive resin (Struers©) as shown in Figure 8b. The yellow marks represent this area of interest, which is located in the centre of the coating.

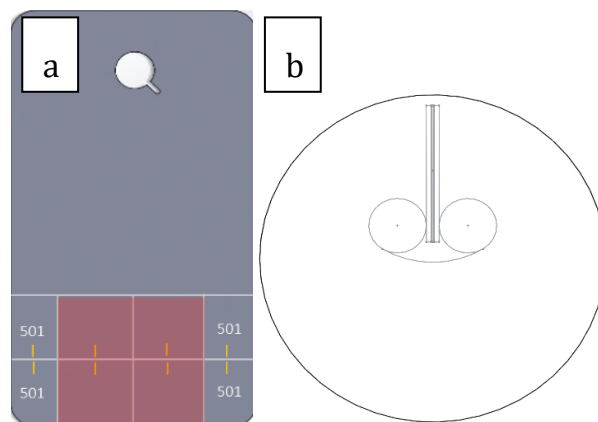


Figure 8: (a) Marking of the samples for cutting, (b) Mounting of the samples for cross-section analysis

The mounted samples are ground with SiC papers of different granulometry from a grit size of P800 (FEPA) to P4000 (FEPA) and then mechanically polished with diamond particles suspension of 3 and 0.5 μm applied on different synthetic clothes.

3.3.2 Characterisation of particles in suspension

Potentiodynamic Polarisation.

The polarisation curve is designed to assess the reduction reaction in the presence or absence of particles. The cathodic curve is consisting of all the ions that are reduced on the cathode. Therefore, the polarisation curve is recorded in the same conditions as the electrodeposition bath (Supplement I – Table 1) but without the metal salts. So, the reduction of nickel would not mask the hydrogen evolution. The polarisation is applied from OCP to cathodic overvoltage equivalent to a current density of 5 A/dm^2 . An Ag/AgCl (3M KCl) reference electrode and a platinum electrode are used as reference and counter electrode, while the working electrode is the same substrate as for the deposition. An IVIUM Vertex potentiostat is used for the electrochemical measurements, and the sweep rate was 2 mV/s .

ζ -Potential measurements and Titration.

As described in the introduction section, the ζ -potential measurements provide information on the potential at the outer Helmholtz layer of the ionic cloud that surrounds the particle because of the adsorption. This adsorption varies with the pH and ion type and concentration in the electrolyte. The ζ -potential of the particles is determined by a Zetasizer Nano ZS (Malvern Instruments, Herrenberg) using the principle of electrophoresis measured by laser Doppler velocimetry. The solution is diluted enough to be translucent to allow the detection of the electrophoretic mobility by an indecent laser beam. The exact dilution is described in Supplement II. The refraction index of the particle is set to 2.610 and the electrolyte adsorption to 0.900. The pH value is adjusted by H_2SO_4 or NaOH , and the particles are kept in suspension by continuous agitation and US for five minutes before measurements.

The ζ -potential is expressed as the average value of three different sets of ten ζ -potential measurements.

Supplement II studies the behaviour of particles as produced and in surface treated state. The buffer capacity of these particles is measured by titration curves, where for a specific volume (60 mL) a known titrator (NaOH 0.01M) is added, and the pH is measured. 20 g/L of SiC particles are added to distilled water, and the pH is measured and then adjusted to pH 3.0 by HCl. The titration is made towards alkalization because in nickel electroplating the cathodic current efficiency is less than 100%. Thus, hydrogen reduction is always expected. Hence, pH tends to increase locally.

3.3.3 Imaging techniques

3.3.3.1 Scanning electron microscopy (SEM) and Electron backscatter diffraction (EBSD)

In SEMs, the electrons are generated in an electron gun and afterwards, focused onto the surface of the sample. When the electron beam scans across the surface, the interaction between the electrons and the atoms in the sample generates emission of different types of signals. The secondary electrons (SE) are the signals used for imaging, and their resolution is dependent on the acceleration voltage and the detector capacity. In this study, the surface morphology is observed by JEOL 7001F - scanning electron microscopy with an acceleration voltage of 15 kV.

EBSD is a characterisation technique that uses the backscattered electrons diffracted into a phosphor screen to form Kikuchi bands which correspond to the lattice diffracting crystal planes [70]. This technique can be used to define grain size and grain shape, grain boundary and grain orientation. Samples have been prepared in cross-section to be analysed by EBSD - EDAX-TSL. The measurements are performed with an electron probe current of approximately 4.4 nA at an acceleration voltage of 15 kV, with a magnification of X6000, and a step size of 80 nm. The OIM 5TM software is used for the analysis of the EBSD maps in the growth direction (perpendicular to the cross-section). All the data points with coefficient index (CI) <0.1 are disregarded. The analysis is performed on two samples for each condition. The grain is defined as a region consisting of at least three similarly oriented connected points with a misorientation <5°. The grain area is calculated by the number of data points contained in this region and the grain diameter by a fitting circle. Because of the spatial resolution of the technique, the SiC- β particles phase is not detected in the EBSD maps, and they can be seen as unindexed (white or black spots) areas when large enough to be recognised.

3.3.4 Non-Imaging techniques

3.3.4.1 Chemical composition by Wavelength-dispersive X-ray spectroscopy (WDS)

As described in the previous section, the SEM generates a series of different types of signals. The electron beam-surface interaction causes the emission of an inner shell electron, thus leaving the atom in an excited state. The inner vacant site is then filled by an outer shell electron, which leads to the relaxation of the atom to its ground state. The energy related to this process is emitted as X-Rays. These X-Ray signals can be collected and used for chemical composition analysis. The number and energy of the

X-rays emitted from the sample can be measured and corresponded it to a chemical element. This technique is referred to as energy-dispersive X-ray spectroscopy (EDS). However, because of the energy level of light elements, such as silicon or low content, the preferred characterisation technique for higher resolution is Wavelength-dispersive X-ray spectroscopy (WDS). Unlike the EDS, WDS reads only the X-rays of a specific wavelength at a time.

The weight % of Si is calculated based on Si pure standards. The analysis of the standard and each specimen is performed using an acceleration voltage of 10 kV and beam current ranging from 14.5 to 18 nA in Supplement I, and 22 nA to 24 nA in Supplement II and III. The volume content of SiC is expressed as the average value of five different WDS area measurements considering Si, and calculated with the assumption that the SiC powders have stoichiometric composition and density of 3.22 g/cm³ at 25 °C.

3.3.4.2 Crystal structure by X-ray powder diffraction (XRD)

X-ray powder diffraction (XRD) is used for phase identification. The phase analysis is performed using a Panalytical X'pert diffractometer using a Cu X-ray tube, a Bragg-Brentano HD optics with a 1/2° divergence slit and a 1/2° antiscatter slit on the incident side, and a 5 mm anti-scatter slit and an X'celerator detector in scanning line mode on the secondary side.

The X-ray diffraction can be also be used for residual stress measurements, which uses the distance between crystallographic planes as a strain gage. These residual stresses can be defined as the stresses which remain in a material in the absence of any external forces, i.e. the internal stress in the Ni grains produced by the parameters of the process, or the codeposition of SiC particles. The deformations caused by the changes in the spacing of the lattice planes compared to their stress-free value will correspond to the magnitude of the residual stress.

The residual stress measurements are performed using the $\sin^2\psi$ -technique using a five-axes cradle on a Panalytical Empyrean diffractometer. The diffractometer is used in a parallel beam configuration with a point-focused copper anode source (Cu K α , $\lambda=0.154$ nm), operating at 45 kV and 40 mA. The primary beam is conditioned by an X-ray lens and 2 x 2 mm² crossed-slits, and in the secondary beam path is used a 0.27° parallel plate collimator. A PIXcel detector is used in 0D mode for the data acquisition. θ -2 θ measurements are performed in a range of 4° around the 400 reflections of Ni for different tilt angles ψ , with $\sin^2\psi$ in the range of 0-0.9. The d-spacing is calculated and plotted as a function of $\sin^2\psi$, and the residual stress is calculated from the slope using Young's modulus ($E = 225.13$ GPa) and Poisson's ratio ($\nu = 0.2956$) for Ni. The residual stress analysis is performed using Panalyticals X'Pert Stress software.

3.3.4.3 Microhardness

The microhardness is done based on the Vickers Hardness test [71], where a pyramidal-shaped indenter leaves a mark on the samples. The vickers hardness number is determined by the load and the dimensions of the mark. The microhardness of the coatings is measured on cross sections by Vickers indenter (NanoTestTM Vantage) with an indentation load of 100 mN and a dwell time of 10 s. Thirty repetitions are done on two samples of each condition, and the microhardness is expressed as the average.

The general rule of mixture of composites [2] is adapted to calculate the theoretical Vicker microhardness of the composite coating based on the fraction of the reinforcer and its hardness. The adapted rule of mixture used in this study states that the hardness of the metal matrix increases as a function of the SiC content:

Equation 1: Microhardness of Composite by an adapted rule of mixture

$$HV_c = fHV_{SiC} + (1 - f)HV_{Ni}$$

Where

$$f = \frac{V_{SiC}}{V_{SiC} + V_{Ni}} \text{ is the volume fraction;}$$

HV_{SiC} is the hardness of SiC (2563 HV)[72];

HV_{Ni} is the hardness of Ni (280 [Suppl. I])

The microhardness is constructed based on the Ni hardness, taken from pure nickel produced under DC 4 A/dm².

SUMMARY OF RESULTS AND DISCUSSION

CHAPTER INTRODUCTION

In this chapter, the main results of the appended papers are summarised and discussed. This chapter is divided into three parts: the interaction of the nanoparticles with the electrolyte, the influence of the process parameters on the nanoparticle content in the coating, and the synergistic effect of the process and particle content on the deposits' microstructure and its impact on the resulting properties of the composite.

4.1 CHARACTERIZATION OF THE SiC PARTICLE- Ni ELECTROLYTE INTERACTION

The characterisation of the interaction between the SiC particles and the Ni electrolyte is treated in Supplements I and II. The results described in this section are used to explain the considerations behind the codeposition of particles recount in this research work.

As mention in the literature review section, the production of composites are very dependent and sensitive to minor changes in the process parameters [24], and can also produce vastly different results based on the selection of the particle [11,12,24]. Even in some cases under the same electroplating conditions, chemically identical particles but with different sizes or from different suppliers produce coatings with different particle content [8,38,72] and final properties. Table 3 summarises the discrepancies in this study.

Table 3: Codeposited SiC volume content (%) under DC and silent agitation as determined by WDS

	SiC 50 nm	SiC 300 nm	SiC 500 nm	SiC 5 μ m
SiC vol.%	0.78	1.78	11.15	3.84
<i>St. dev</i>	<i>0.13</i>	<i>1.06</i>	<i>1.15</i>	<i>0.25</i>

Even if the same nominal size is selected, when comparing different studies on additive-free electrolytes, particles with identical size also show variations in the codeposition [12,38,54,56,73,74]. As described in multiple studies [32,36,67,75,76], the responsibility for such differences is the role that the electrolyte plays in the behaviour of the particle while in suspension, determined by ζ -potential measurements. However, this behaviour is often described but not fully understood.

Previous studies done on SiC nanoparticles, described a negative ζ -potential of nano-SiC particles at pH 4.5 in an additive-free Watt's-Co bath [66], at pH 4 in a modified Watt's bath [65], and at pH 3 in NaCl 0.01M [33] whereas it was positive at similar pH in different electrolytes [32,36,63]. The ζ -potential analysis of the particles used in this study shows a deviation of a few millivolts difference between sizes; all values are negative and close to zero at pH 3 (Table 4)

Table 4: ζ -potential of as produced SiC particles (0.2 g/L) in diluted (25%) Watt's bath at pH 3

	SiC 50 nm - AP	SiC 300 nm - AP	SiC 500 nm - AP	SiC 5 μ m - AP
ζ-potential	-0.30	-2.29	-5.54	-0.07
<i>St. dev</i>	0.74	0.72	0.69	0.89

From these results, it can be established a correlation between the ζ -potential measurements and the deposition rate reported in Table 3. A high absolute ζ -potential value increases the particle content. Nevertheless, theoretically the codeposition should decrease at negative values since the cathode is charged negatively too; thus, the electrophoretic transport should not be possible. However, another study [66] also reported SiC codeposition even if the ζ -potential negative. The author even described a maximum deposition in more negative values by the use of SDS as an additive.

It is presumed the futility of ζ -potential values to explain the codeposition. The characteristics of the ζ -potential technique limit the validity of the results. As described in the characterisation section, the ζ -potential technique depends on the dilution of the electrolyte to allow the incident beam to detect the electrophoretic mobility of the particles. Consequently, the ζ -potential values are not representative of the real electroplating conditions. Thus, the adsorption that the particle experiences in the real electrolyte will vary and could modify the sign of the ζ -potential, explaining why the codeposition varies between sizes. Supplement II analyses these results in depth.

It has been studied the particle's surface interaction with the chemical surroundings and identified its critical role in the codeposition [24,31]. The electrodeposition of composites is based on the assumption that the particles are pure. However, the particles' behaviour is not always consistent, pointing to differences in the surface state. Supplement I discusses the results from a polarisation test in a solution that contains only the particles in distilled water at pH 3. Figure 9 shows how these particles with the same theoretical composition interact differently with the solution when a cathodic overpotential is applied. The curves show a shift in the reduction potential of free H^+ . The simple presence of particles changes the reduction rate compared to the water electrolysis.

Table 5: Distilled- H_2O pH after addition of the as produced particles

H_2O pH ₀	SiC 50 nm-AP	SiC 300 nm-AP	SiC 500 nm-AP	SiC 5 μ m-AP
~6.0 pH after addition	8.07	5.17	3.03	5.89

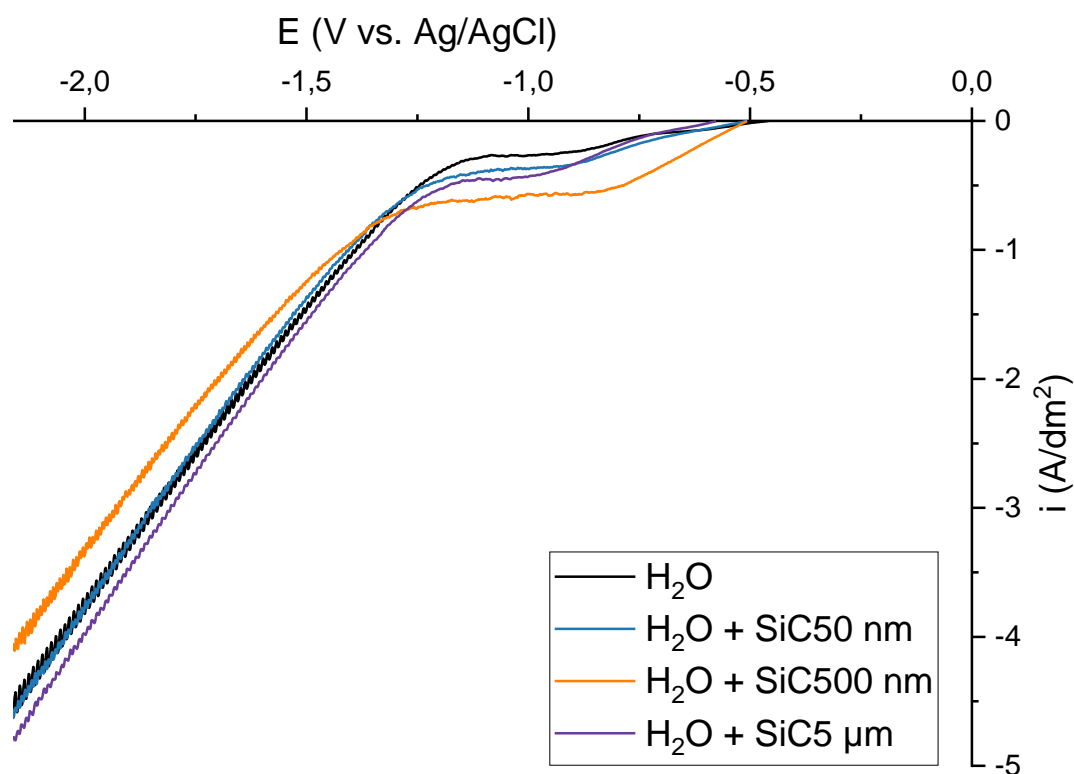


Figure 9: Polarization curves of particles and electrolytes without Ni salts. Adapted from Supplement I.

It is presumed that the SiC 50 nm particles have a strong H^+ surface adsorption [31], shown by the increase in pH when added to water (Table 5). When the particles are in the vicinity of the cathode during the polarisation test, this adsorption will perturb the reduction rate of the electrolyte's free H^+ . The shift in the hydrogen rate in the presence of SiC 5 μm could be due to the shielding effect over the cathode surface because of the larger non-conductive particles. Nevertheless, the shift is more pronounced in the solution with the SiC 500 nm particle. Supplement I and II discuss the hypothesis of surface impurities that decreases the pH. The nature of the impurities are unknown, but this presumably will acidify the solution, decreasing the pH as reported in Table 5. Therefore, the reduction rate detected in the polarisation test is no longer only the reduction of the electrolyte's hydrogen, but also the reduction of any H^+ present due to the particles.

Supplement II discusses even further how distinct is the particle-electrolyte interaction for each size (50 nm, 300 nm, and 500 nm) in the as-produced state. Titration (Figure 10) is carried out with the particles in suspension in water. The titration curves show different behaviours, thus pointing to a difference in the surface reactivity between particles. As-produced (AP) SiC50 and SiC300 curves are different from water's curves; requiring at least 30% more titrator to reach the same pH. Although, both have a gentle pH slope change. A mild buffering effect is observed in these particles since there is a delay in the curve slope and a difference in the pH stabilisation plateau. In the cases of SiC50 and SiC300, as previously discussed, it may well be due to the hydrogen adsorption [31] that is released from the surface acting as a buffering agent. The buffering effect in SiC300 is sufficient to the delay in the stabilisation plateau but lower compared to SiC50.

On the contrary, SiC500 titration curve showed a strong buffering effect. The pH remained stable for the all titrator content range. As suggested in the Supplement II discussion, this is presumably due to the strong presence surface impurities or its ionic species, which would act as buffer agents in addition to H^+ adsorption.

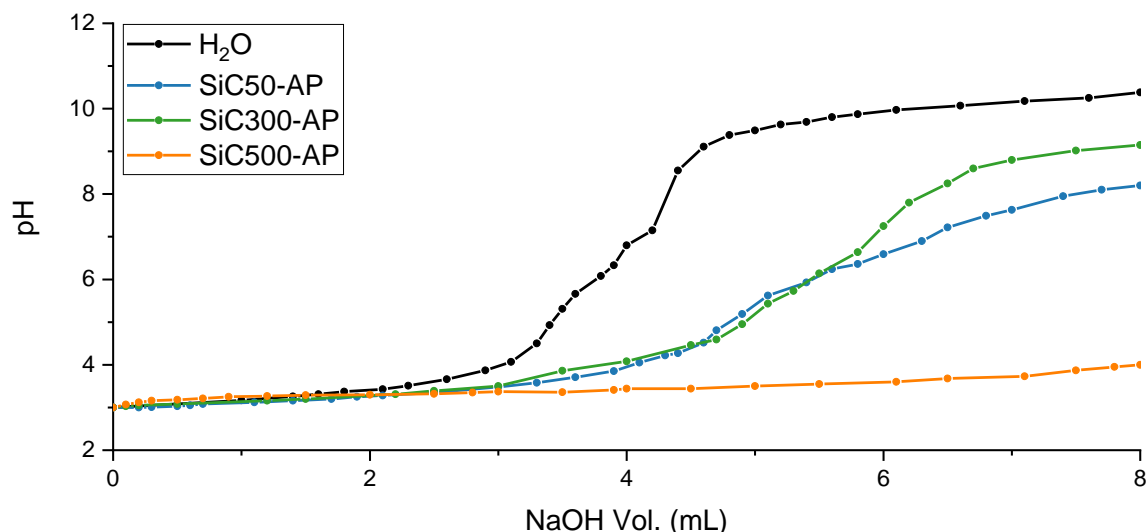


Figure 10: Titration curves (NaOH 0.01M) on 60 mL volume of H_2O and as produced 20 g/L SiC particles. Adapted from Supplement II.

These studies discussed the hypothesis that the particles' interaction is unpredictable because of the unknown differences on the particle surface, leading to different types of interaction which depend on the surface state of the particle.

In order to control the production process, Supplement II proposes a surface treatment designed to remove possible impurities and consistently oxidise the particles' surface to set a common surface state on the nano- and submicron-particles despite any initial state. This is done without modifying the electrolyte formulation, i.e. no additives are added. Table 6 shows how the ζ -potential of all the particles is stabilised around -1 mV (Fig. 2). Therefore, it is supposed that the pre-treatment effectively established a common surface state. Nevertheless, due to the limitations of the ζ -potential technic, it is not possible to confirm that the mechanisms of the particle-electrolyte interaction are modified.

Table 6: ζ -potential of surface treated SiC particles (0.2 g/L) in diluted (25%) Watt's bath at pH 3

	SiC 50 nm - ST	SiC 300 nm - ST	SiC 500 nm - ST
ζ-potential	-1.17	-0.88	-1.70
<i>St. dev</i>	1.02	0.44	0.55

Likewise, the titration is carried in the same conditions as for the as-produced particles. Because of the surface oxidising induced by the surface treatment, it is presumed that any impurity is removed and surface adsorption modified, and instead, a thin film of silicon dioxide covers the particles' surface to some extent. This allows less partial adsorption of OH^- or H^+ which decreases the buffer effect on all the sizes (Figure 11). The titration curves in all cases are shifted closer to water, and the

slope change occurred with less addition of NaOH. This shows that even if the state of the particles' surface is unknown, the surface treatment successfully brings the SiC particles independently of their size, batch, production route to a common surface state and a soft interaction with the electrolyte.

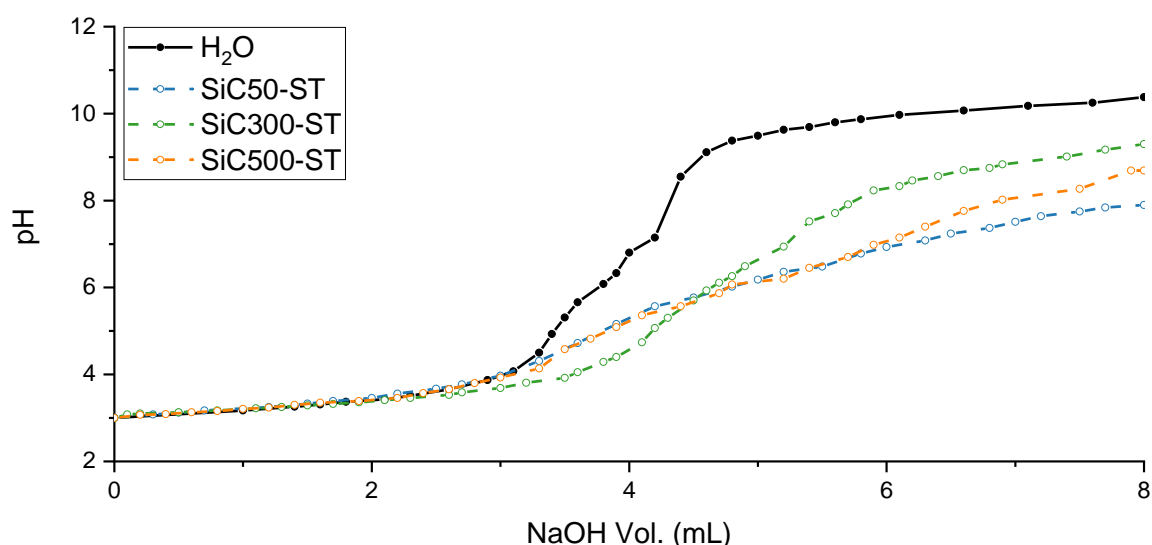


Figure 11: Titration curves (NaOH 0.01M) on 60 mL volume of H₂O and surface treated 20 g/L SiC particles. Adapted from Supplement II.

4.2 ELECTROCODEPOSITION AND SiC PARTICLE

The samples in Supplement I are produced under mechanic (silent) and US agitation, while in Supplement II the particles are surface treated before the electrodeposition. All the samples are produced with the same current density. Figure 12, compares the EBSD maps of as produced SiC500, SiC500 under US agitation, and surface treated SiC500 under silent agitation. This comparison is only done in the SiC 500 nm samples. These particles codeposited in a larger volume compared to the other sizes (Table 7 and Suppl. I – Table 2 and Suppl. II – Table 3), and their nominal size allows the analysis under the SEM. Nevertheless, all the EBSD maps, particle distribution and codeposition analysis are discussed in Supplements I and II.

Table 7: Codeposited SiC500 volume content (%) under DC4 as determined by WDS

	SiC 500 AP - Sil	SiC 500 AP - US	SiC 500 ST - Sil
SiC vol. %	11.15	4.37	19.32
<i>St. dev</i>	1.15	0.17	4.00

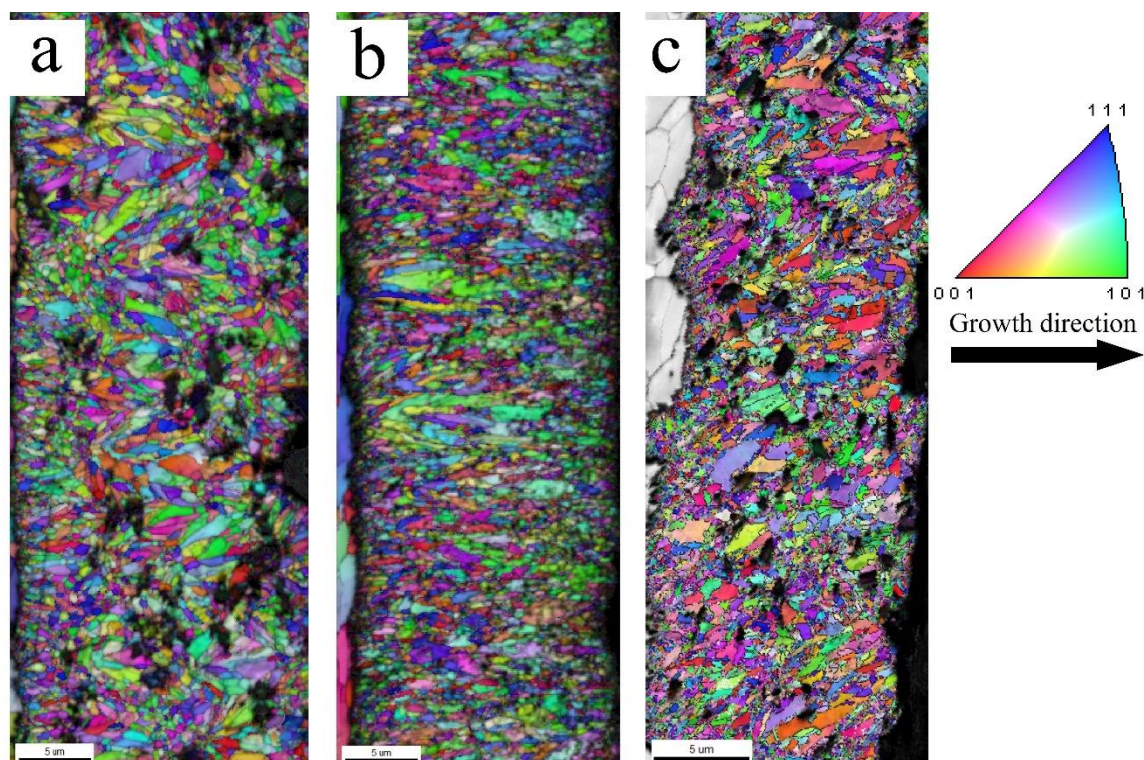


Figure 12: EBSD maps, color-coded in relation to the electrodeposits' growth direction, shown by an arrow in the legend. (a) SiC500 nm as produced and silent agitation, (b) SiC500 nm as produced and US agitation, and (c) SiC500 nm surface treated and silent agitation.

The codeposition rate of the SiC500 under silent stirring is around 11% vol. content, similar to the results reported in previous studies [11,77]. These particles are highly agglomerated (Figure 12a), likely because particles tend to aggregate when the van der Waals forces of attraction are larger than the electrostatic repulsive force [78]. It is discussed in Supplement II, the possible presence of surface impurities and the surface adsorption of H^+ that could encourage a higher attraction between particles because of the likeliness of sharing hydrogen bonds. These van der Waals attractions are broken by the ultrasound irradiation [46], leading to a deagglomeration of the particles (Figure 12b). However, in systems where the US horn is directly placed in the electrolytic bath, and the surface cathode remained unshielded and exposed to the cavitation. This may cause the larger particles to collide and 'bounce' away from the electrode or to be removed from the surface by the cavitation before being anchored in the growing surface [79]. This may have caused a decrease in the particle content, compared to silent agitation (Table 7).

The use of US agitation in an industrial setup could be limited because of the size of the electroplating tanks, and the distribution of the acoustic streaming. Supplement II discusses the impact of the surface treatment on the distribution of particles, maintaining the silent agitation. Figure 12c shows a better distribution compared to the as produced particles electrodeposited under the same conditions. Moreover, the surface treatment encouraged a higher codeposition (Table 7) without prompting an increase in agglomeration. This could be due to a decrease in the van der Waals attraction forces because of the removal of any impurity by the surface treatment, modifying the surface adsorption.

4.3 PULSE ELECTRODEPOSITION OF COMPOSITE COATINGS

Supplement III studies the influence of the current on the codeposition and entrapment of SiC 50 nm particles. It is proposed a modified pulse-reverse current scheme, inspired by the work of Podlaha et al. [59,62] and Xiong-Skiba et al. [60], and modified based on the technique used by Aroyo et al. [80] to avoid the passivation of the anode. This is treated in deep in Supplement II.

Different SiC50 composites are produced under direct current (DC) at 4 A/dm² and 10 A/dm² which corresponds to the average current densities and cathodic of the PR plating, respectively, and under two pulsed-currents: a short-pulse (1 ms cycle) and a adjusted long-pulse. The proposed pulse-reverse waveform would plate a thickness equivalent to the diameter of the particle (50 nm) during the cathodic cycle, and strip half of it during the anodic cycle. The codeposition of the deposits done by this method exceeds the vol. % content when it is benchmarked to the traditional DC and PR methods (Table 8).

Table 8: Codeposited SiC volume content (%) under DC and PP as determined by WDS

	SiC 50 DC4	SiC 50 DC10	SiC 50 PR-SP	SiC 50 PR-LP
SiC vol.%	0.78	1.90	2.07	4.07
<i>St. dev</i>	<i>0.13</i>	<i>0.51</i>	<i>0.30</i>	<i>0.51</i>

The composites produced under DC at 10 A/dm² have a low particle content, close to 2 vol.%, similar to the one reported by Lee et al. [43] at the same pH. Nonetheless, the codeposition is more than doubled compared to DC at 4 A/dm². This could be due to a more rapid entrapment of the particles because of the faster-growing metal as the result of a higher current density. Similarly to the results reported by Gyftou et al. [56], the short pulses do not support the enrichment of the cathode surface. Consequently, the samples produced under PR-SP only increased slightly the particle content. The SiC content is maximum when the samples are produced by a cathodic pulse where the deposits' thickness per cycle approached the particles diameter size. It is presumed that electroplating a thickness which resembles the particle's diameter, will initially capture some of the particles that are in contact with the cathode by the growing of the first metal layer. Since the stripping is half of this thickness, only a few of the entrapped particles are released back to the electrolyte. The anodic pulse train prevents the escape of the particles by maintaining the attraction force to the cathode surface by shifting the current between anodic and cathodic. The next plating cycle captures the nearby particles, without losing the already entrapped particles. Thus, the increase in the SiC vol.% content can be attributed mainly to this technic. Supplement II – Figure 5, offers a description of this technique in detail.

4.4 CODEPOSITION OF SiC AND ITS INFLUENCE IN Ni ELECTROCRYSTALLISATION

This section offers a summary from Supplements I, II, and III and discusses the resulting microstructure of the Ni matrix, and the influence that particles with different sizes, and characteristics enforce onto the electrocrystallisation. Tables 9, 10 and 11 recaps the most relevant results, focusing on nano- and submicron-particles. The perturbation of the electrocrystallisation is supposed to happen in orders of magnitude smaller than microparticles; thus, excluding Ni/SiC 5 μm composites. However, these results are treated in Supplement I.


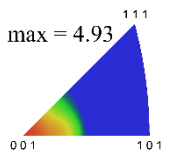
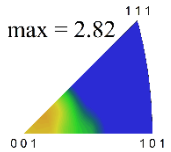
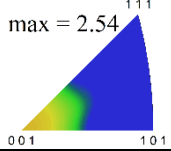
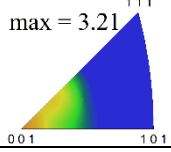
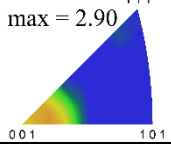
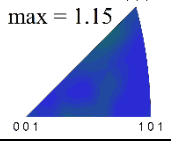
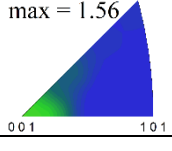
Table 9 presents how particles with different sizes influence the electrocrystallisation of nickel. Even though the metal crystallises under the same current density, the grain size and preferential growth orientation vary for each composite. It is suggested that this variation is due to a double effect caused by the presence of particles. Firstly, the content of SiC decreases the grain size of the matrix, as it has also been suggested in previous studies [38,73,81]. The highest grain refinement is achieved by the highest codeposition rate. The Ni/SiC500 composites achieved a nanocrystalline structure, having a grain size area as low as 0.38 μm^2 . When the SiC content is around 2% the grain size is almost halved compared to the pure Ni deposit, and despite the low content in the Ni/SiC50 samples the grain size is also reduced. From these results, it is presumed a relation between content and size, and the nucleation rate. The particle itself could act as a nucleation site, or due to their non-conductive nature induce a shielding effect which would increase the current density in its surrounding. This will cause an increase in the local current density, increasing the nucleation rate of the metal.

Lastly, the presence of particles modifies the preferential growth of the deposits. The basis of such change may well be the influence that the particles have on the reduction of the metal, i.e. current efficiency and growth inhibition.

As discussed in previous sections, it is presumed that as-produced particles have a surface adsorption of H^+ and a thin surface layer composed of impurities. The hydrogen will be transported to the cathode surface by the particles leading to an increase in the hydrogen evolution, increasing the pH after electroplating. This causes a reduction in the current efficiency and some inhibition in the Ni crystal growth. However, this effect on hydrogen evolution is decreased after the surface treatment. The variation in pH is stabilised around 0.12 in all the composites with surface treated particles.

Furthermore, the inhibition in these samples remained; pointing that the preferential crystal growth is also modified by the particle codeposition. The multiple nucleation sites prompted by the particles, lead to a microstructure that does not allow the normal nickel growth of larger columns. Therefore, leading to the nucleation taking place on atomic planes, so more randomly oriented grains are grown.

Table 9: Recaps of the deposits' variation in pH after electroplating (ΔpH), SiC vol.% content, grain size (area) of the matrix, and crystal orientation represented by the inverse polar figure and crystal orientation frequency. Comparison of Ni/SiC composites under DC4.

	ΔpH	SiC vol.%	GS (μm^2)	 Crystal orientation
Ni – DC4	0.04 ± 0.01	-	4.55 ± 0.24	 max = 4.93
SiC50 – DC4	0.10 ± 0.03	0.78 ± 0.13	3.49 ± 0.21	 max = 2.82
SiC50/ST – DC4	0.12 ± 0.01	1.74 ± 0.35	2.72 ± 0.20	 max = 2.54
SiC300 – DC4	0.19 ± 0.01	1.78 ± 1.06	2.15 ± 0.38	 max = 3.21
SiC300/ST – DC4	0.12 ± 0.01	7.41 ± 1.65	2.25 ± 0.38	 max = 2.90
SiC500 – DC4	0.21 ± 0.03	11.18 ± 1.15	0.38 ± 0.08	 max = 1.15
SiC500/ST – DC4	0.12 ± 0.02	19.32 ± 4.00	0.40 ± 0.08	 max = 1.56

Likewise, Table 10 presents how particles with different sizes influence the electrocrystallisation of nickel under US agitation. Pure nickel deposits experienced a reduction in the grain size compared to the silent agitation, in agreement with previous studies [48,82]. This is due to an increase in the number of finer grains along the larger columnar grain (Supplement I – Figures 3 and 6). Comparable to the samples produced under silent agitation, the presence of particles causes a grain refinement in the metal matrix. The combination of the refinement of the metal caused by US and the better dispersion of the particles led to a finer microstructure. The US agitation slightly increased the pH variation, although this increase in the hydrogen evolution had no impact on the preferred grain orientation growth.

The composites produced under US agitation experienced an increased in the crystal orientation frequency index in favour of the [100] crystal growth. It is presumed that the strong acoustic agitation produced by US not only caused a better dispersion of the particles but also removed some of the inhibiting species from the cathode's surface decreasing the growth inhibition. This is further discussed in Supplement I.

Table 10: Recaps of the deposits' variation in pH after electroplating (ΔpH), SiC vol.% content, grain size (area) of the matrix, and crystal orientation represented by the inverse polar figure and crystal orientation frequency. Comparison of Ni/SiC composites under DC4 and US agitation.


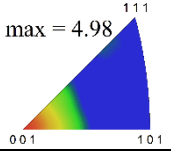
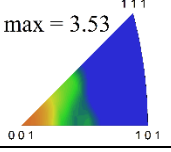
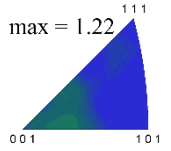

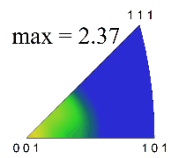
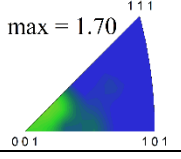
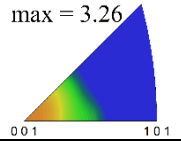
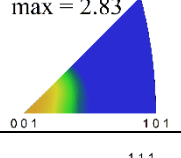
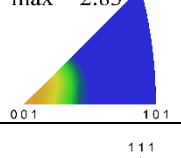
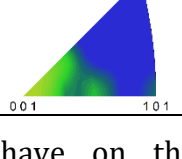
	ΔpH	SiC vol.%	GS (μm^2)	 Crystal orientation
Ni – DC4/US	0.07 ± 0.01	-	2.92 ± 0.16	 max = 4.98
SiC50 – DC4/US	0.12 ± 0.03	2.67 ± 0.54	2.77 ± 0.15	 max = 3.53
SiC 500- DC4/US	0.28 ± 0.03	4.37 ± 0.17	0.42 ± 0.08	 max = 1.22

Table 11 presents a summary of the deposits' produced under different current parameters. Ni under DC10 had the highest grain refinement, due to the increase of nucleation rate over the growth as described in the introduction section. The PR had a lower grain refinement compared to these samples since the average current density is lower than in DC10. Thus, the samples are more comparable to the Ni deposit produced under DC4, which current density corresponds approximately to the total average current density [23]. The use of PR currents somewhat refines the microstructure by increasing the number of smaller grain (Supplement II – Figure 6).

The increase in pH varies between plating techniques due to the difference in electroplating time (Supplement II – Table 1). The longer plating time in PR-LP caused the highest change in pH. Compared to pure Ni under DC4 (Table 9), this increase in pH provoked a decrease in the preferred orientation growth. However, it is in a lower quantity compared to pure Ni under DC10. It is supposed that the higher number of nucleation sites contributed to more random deposits.

A comparison between pure Ni and composites shows a consistent increased in pH in the production of the latter. This strengthens the assumption that the presence of particles modifies the reduction of hydrogen by the nature of the adsorption at their surface. Additionally, the codeposition also modifies the preferential growth by the triple mechanism of inducing an inhibited growth, because of the already mention surface adsorption, an increase in the hydrogen evolution, and the proclivity of inciting nucleation on atomic layer leading to randomised crystal orientations.

Table 11: Recaps of the deposits' variation in pH after electroplating (ΔpH), SiC vol.% content, grain size (area) of the matrix, and crystal orientation represented by the inverse polar figure and crystal orientation frequency. Comparison of Ni/SiC50 composites under DC10, PR-SP and PR-LP

	ΔpH	SiC vol.%	GS (μm^2)	 Crystal orientation
Ni – DC10	0.02 ± 0.02	-	1.06 ± 0.13	 max = 2.37
SiC50 – DC10	0.10 ± 0.02	1.90 ± 0.51	0.81 ± 0.12	 max = 1.70
Ni – PR-SP	0.08 ± 0.03	-	3.42 ± 0.17	 max = 3.26
SiC50 – PR-SP	0.13 ± 0.02	2.07 ± 0.30	1.24 ± 0.20	 max = 2.83
Ni – PR-LP	0.55 ± 0.05	-	2.20 ± 0.18	 max = 2.83
SiC50 – PR-LP	0.65 ± 0.05	4.07 ± 0.51	2.41 ± 0.19	 max = 1.99

The preceding tables showed the effect that the particles have on the electrocrystallisation. Not only is affected the arrangement of the Ni atoms within the crystal lattice, changing the grain orientation but also in some cases, the codeposition also modifies the microstructure leading to finer structures. The latter will have a strong effect on the final properties of the composite coating since it will cause a Hall-Petch strengthening on the deposits. Moreover, the composites will also be hardened by the fraction of codeposited SiC reinforcer. Thus, the synergistic effect of the interactions between particle, current, and electrocrystallisation will undeniably affect this combined hardening. It is difficult to attribute which relationship is more critical for this effect since the selection of the current will alter the electrocrystallisation of the matrix, which in turn is also modified by the particle codeposition, that also varies with the current, and bath setup. Figures 14 and 15 attempts to open for analysis this relationship for by plotting the deposits' hardness against the strengthening caused by grain refinement, and by the SiC codeposition.

Figure 14 points a relationship between hardness and grain size for pure Ni. A black-dashed line is plotted to represent the refinement of pure Ni, extrapolated starting only from two experimental points: Pure Ni under DC4 and DC10. These two values are representative of a large columnar microstructure and the most refined grain size. The rest of the pure Ni values (black-coded) can be accommodated within the line, manifesting a hardness-grain size relationship. Some of the values achieved by the composite coatings can also be accommodated within this line, except for SiC50 produced by PR-LP, surface treated SiC500, and SiC500 under US agitation. The fact that some of the composites follow a similar linear relationship as the one seen in pure Ni. Points out that the changes in the electrocrystallisation because of the codeposition increases the hardness in these samples, i.e. by the resulting microstructure, and not by the particle content alone.

Although the grain refinement in the SiC50 composite produced under PR-LP is far from the one reported by DC10, the increase in hardness is higher, evidencing that the hardening effect is due to the codeposition. However a synergistic effect is to be highlighted: hardening is not only due to the particle content but also because of the particle-current interaction, given by effect that the PR-LP waveform has on the grain growth and probably on the particle anchoring. It is presumed this method would dissolve small nuclei equal to the stripping mass during the anodic pulse, leaving only the bigger grains with partially entrapped particles, as it is designed with this goal. Then, these grains will continue to grow during the next cathodic pulse, covering the particles in a single grain completely.

The highest hardness is attained by the codeposited SiC 500 nm. However, SiC500 under DC4 can be accommodated within the Hall-Petch strengthening line. Comparing this composite to surface treated SiC500, and SiC500 under US agitation, it shows that hardness in these two coatings is to the increase in the particle content on the first, and the better distribution achieved by US on the latter. Therefore, in these composites, the total hardness of the deposits is a function of the synergistic effect between microstructure and particle content.

Figure 15 portrays the deposits' hardness and SiC fraction related to an adapted rule of mixture that intends to define the role that particle content plays in the hardness. As discussed in the Research Approach section, the hardness of the composite is calculated by accounting the contribution that the SiC particles have on increasing the hardness of Ni, represented by the black-dashed line. The composite hardness for each sample is recalculated using Equation 1 and included in Figure 15.

Some of the composites, but not all of them, fit within the line. This shows that even when a high hardness is attained, the poorly distributed and agglomerated particles hinder the coatings' final properties. This is especially recognized in SiC500 where a poor distribution (Figure 12a) decreased hardness. On the contrary, the surface treated SiC500, and SiC500 under US agitation that due to their better particle distribution (Figure 12) attained higher hardness. Likewise, SiC50 produced by PR-LP also achieved a greater hardness because of the better particle distribution as a consequence of the characteristics of the production method. The increase in hardness on SiC50 DC10 is explained by the differences in the microstructure compared to the nickel hardness taken from Pure Ni by DC4 from which the composite hardness is constructed.

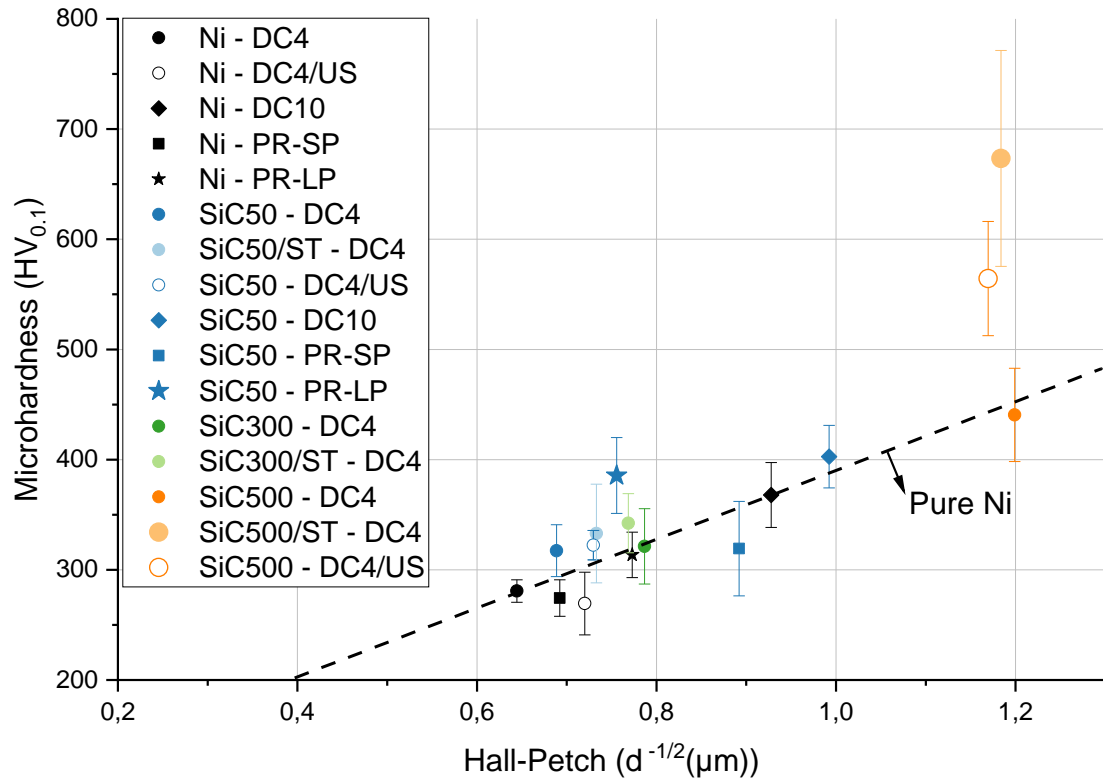


Figure 14: Microhardness vs Hall-Petch grain size relationship for the samples listed in tables 9, 10, and 11. The increase in hardening in pure Ni is indicated by the black-dashed line.

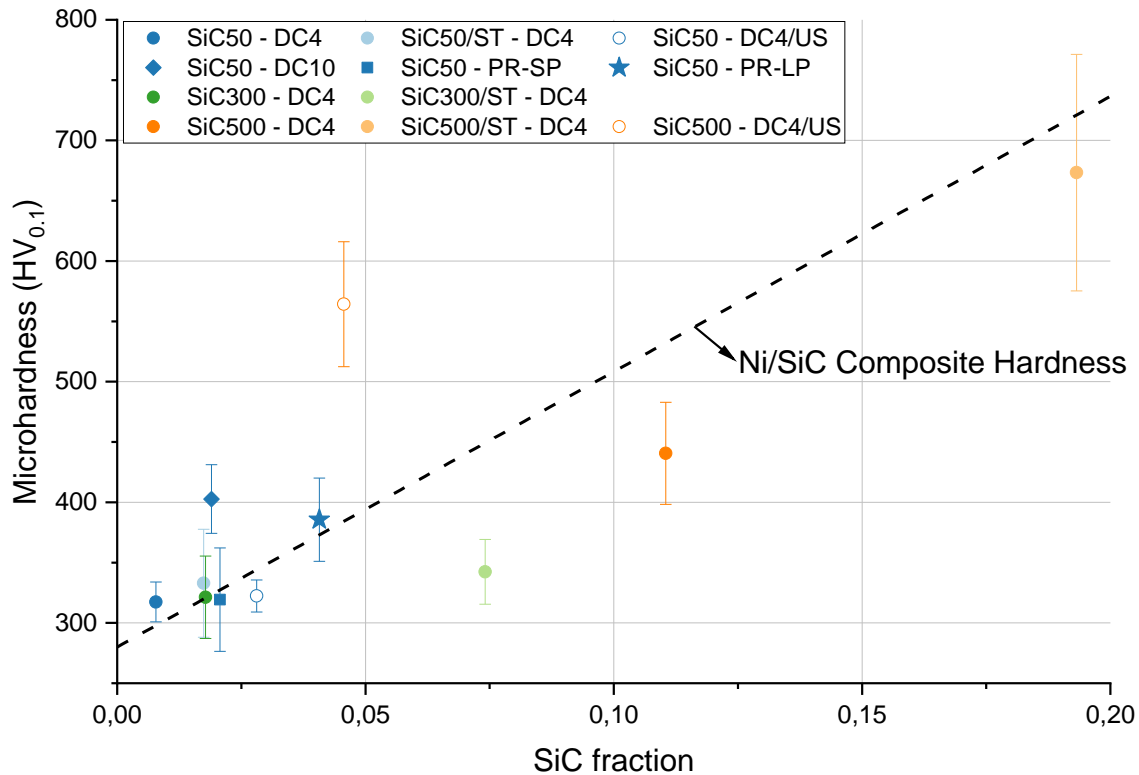


Figure 15: Adapted rule of mixture. Microhardness vs SiC codeposited fraction relationship for the samples listed in tables 9, 10, and 11.

CONCLUSIONS

CHAPTER INTRODUCTION

In this chapter, some conclusions have been drawn based on the results.

The understanding of the mechanisms governing the codeposition process of the reinforcer phase and their influence on the electrocrystallisation of the metal matrix in composite electroplating is of major importance to predict and tailor the final performance of the coating. This study introduced the microstructural characterisation of composite coatings with different particle size, promoting a better understanding of the interactions between particle, current, and electrocrystallisation of the metal. The following conclusions are highlighted:

PARTICLE-ELECTROLYTE INTERACTION

The inconsistency in the behaviour of particles with the same composition is due to the presence of unknown impurities on their surface. These differences in the surface state were confirmed by ζ -potential measurements, titration curves, and polarisation tests. It was proposed a surface treatment based on HNO_3 which successfully brought the particles independently of their size to a common state, proved by closer values in ζ -potential and behaviour in the titration curves.

The change in this particle-electrolyte interaction by the surface treatment benefit the dispersion of the particles, leading to an increase in the codeposition rate which in some cases was doubled or tripled.

PARTICLE-CURRENT INTERACTION

It was proven successful that a pulse-reverse waveform can be designed to increase the content of codeposited nanoparticles. The composite produced by this method doubled the vol.% content of nanoparticles compared to other methods, also leading to a noticeable increase of the hardness.

PARTICLE-ELECTROCRYSTALLISATION INTERACTION

Build upon the analysis of different interactions. A synergistic effect between particle and electrocrystallisation was identified, which affected the final properties of the coating. It was possible to define a relationship between particle, and the resulting microstructure due to both the codeposition and current input.

The codeposition of particles promoted an increase in the nucleation rate, encouraging a grain refinement independently of the current. The study of the particle influence on the metal microstructure showed that particles do not only reinforced the composite by their fraction, but also by modifying the metal microstructure during electrocrystallization. Two technique proved to be successful in reducing the agglomeration, the ultrasonic agitation and the surface treatment. The pulse-reverse technique was also successful in producing well-dispersed nanocomposites.

FUTURE WORK

CHAPTER INTRODUCTION

In this chapter, some ideas are presented on how to continue the future work.

Various directions can be considered as future routes to exploit and improve the knowledge acquired in this study. The findings of this work can be extended in future work by exploring the codeposition of different type of nanoparticles or variations in the electrolyte formulation.

To better understand the origin of the particles surface impurities or chemical state XPS should be applied to the nanopowder in different states: as produced, after the surface treatments and after immersion in the deposition bath. This characterisation, connected to the powder analysis before rinsing, will provide information on what compounds are released, if any, into the electrolyte. Finally, the XPS characterisation of the surfaced treated particle would point to what is the final surface state after the treatment and reason the increase of codeposition and dispersion of these particles.

TEM analyses should be applied to the pulse reverse deposits to observe where the nanoparticles are preferentially embedded compared to the metal microstructure. This could prove if the specific pulse-reverse long pulse waveform can control the particle embedding within the growing grain.

Even further tailoring of the pulse-reverse long pulse method can be developed by modifying the parameters with the goal of finding the optimal set-up. This includes increasing periods of plating and stripping, experimenting with different particle size, or particle composition.

This new collected knowledge should be tested on systems different from Ni/SiC to prove that developed knowledge is independent of the specific experimental conditions and chemistry. As different particle size have a different impact on the metal layer, a dual system can be developed coating a mixture of different particles.

REFERENCES

- [1] W.D. Callister, D.G. Rethwisch, Materials science and engineering, 9th ed., Wiley, Hoboken, NJ, 2015.
- [2] M.F. Ashby, Materials selection in mechanical design, 4th ed., Elsevier/Butterworth-Heinemann, Amsterdam, 2011.
- [3] European Chemicals Agency, Substances restricted under REACH. echa.europa.eu/substances-restricted-under-reach.
- [4] M. Lekka, C. Zanella, A. Klorikowska, P.L. Bonora, Scaling-up of the electrodeposition process of nano-composite coating for corrosion and wear protection, *Electrochim. Acta* 55 (2010) 7876–7883.
- [5] P. Gyftou, E.A. Pavlatou, N. Spyrellis, K.S. Hatzilyberis, Nickel Matrix Composite Coatings, *Trans. IMF* 78 (2000) 223–226.
- [6] Y.D. Gamburg, G. Zangari, Theory and Practice of Metal Electrodeposition, Springer Science+Business Media LLC, New York, NY, 2011.
- [7] J.R. Roos, J.P. Celis, J. Fransaer, C. Buelens, The development of composite plating for advanced materials, *JOM* 42 (1990) 60–63.
- [8] P. Gyftou, M. Stroumbouli, E.A. Pavlatou, P. Asimidis, N. Spyrellis, Tribological study of Ni matrix composite coatings containing nano and micro SiC particles, *Electrochim. Acta* 50 (2005) 4544–4550.
- [9] M.R. Vaezi, S.K. Sadrnezhaad, L. Nikzad, Electrodeposition of Ni–SiC nano-composite coatings and evaluation of wear and corrosion resistance and electroplating characteristics, *Colloids Surf., A* 315 (2008) 176–182.
- [10] D. Thiemig, A. Bund, Characterization of electrodeposited Ni-TiO₂ nanocomposite coatings, *Surf. Coat. Technol.* 202 (2008) 2976–2984.
- [11] T. Lampke, A. Leopold, D. Dietrich, G. Alisch, B. Wielage, Correlation between structure and corrosion behaviour of nickel dispersion coatings containing ceramic particles of different sizes, *Surf. Coat. Technol.* 201 (2006) 3510–3517.
- [12] C. Zanella, M. Lekka, P.L. Bonora, Influence of the particle size on the mechanical and electrochemical behaviour of micro- and nano-nickel matrix composite coatings, *J. Appl. Electrochem.* 39 (2009) 31–38.
- [13] E. Budevski, G. Staikov, W.J. Lorenz, Electrocrystallization, *Electrochim. Acta* 45 (2000) 2559–2574.
- [14] J. Amblard, I. Epelboin, M. Froment, G. Maurin, Inhibition and nickel electrocrystallization, *J. Appl. Electrochem.* 9 (1979) 233–242.
- [15] R. Winand, Electrocrystallization - theory and applications, *Hydrometall.* 29 (1992) 567–598.
- [16] K. Raghunathan, R. Weil, The effects of some plating variables on the structure of thin nickel electrodeposits, *Surf. Technol.* 10 (1980) 331–342.

- [17] A. Vicenzo, P.L. Cavallotti, Structure and electrokinetic study of nickel electrodeposition, *Russ. J. Electrochem* 44 (2008) 716–727.
- [18] T.J. Mason, A.J. Cobley, J.E. Graves, D. Morgan, New evidence for the inverse dependence of mechanical and chemical effects on the frequency of ultrasound, *Ultrason. Sonochem.* 18 (2011) 226–230.
- [19] C. Kollia, N. Spyrellis, J. Amblard, M. Froment, G. Maurin, Nickel plating by pulse electrolysis, *J. Appl. Electrochem.* 20 (1990) 1025–1032.
- [20] O.P. Watts, Rapid nickel plating, *Trans. Am. Electrochem. Soc.* 29 (1916) 395–403.
- [21] A.M. Rashidi, A. Amadeh, The effect of current density on the grain size of electrodeposited nanocrystalline nickel coatings, *Surf. Coat. Technol.* 202 (2008) 3772–3776.
- [22] R. Vittal, H. Gomathi, K.-J. Kim, Beneficial role of surfactants in electrochemistry and in the modification of electrodes, *Adv. Colloid Interface Sci.* 119 (2006) 55–68.
- [23] M.S. Chandrasekar, M. Pushpavanam, Pulse and pulse reverse plating—Conceptual, advantages and applications, *Electrochim. Acta* 53 (2008) 3313–3322.
- [24] C.T.J. Low, R.G.A. Wills, F.C. Walsh, Electrodeposition of composite coatings containing nanoparticles in a metal deposit, *Surf. Coat. Technol.* 201 (2006) 371–383.
- [25] N. Guglielmi, Kinetics of the Deposition of Inert Particles from Electrolytic Baths, *J. Electrochem. Soc.* 119 (1972) 1009–1012.
- [26] J.P. Celis, J.R. Roos, C. Buelens, A Mathematical Model for the Electrolytic Codeposition of Particles with a Metallic Matrix, *J. Electrochem. Soc.* 134 (1987) 1402–1408.
- [27] J. Fransaer, J.P. Celis, J.R. Roos, Analysis of the Electrolytic Codeposition of Non-Brownian Particles with Metals, *J. Electrochem. Soc.* 139 (1992) 413–425.
- [28] B.J. Hwang, Mechanism of Codeposition of Silicon Carbide with Electrolytic Cobalt, *J. Electrochem. Soc.* 140 (1993) 979.
- [29] P.M. Vereecken, I. Shao, P.C. Searson, Particle Codeposition in Nanocomposite Films, *J. Electrochem. Soc.* 147 (2000) 2572.
- [30] P. Berçot, E. Peña-Muñoz, J. Pagetti, Electrolytic composite Ni-PTFE coatings, *Surf. Coat. Technol.* 157 (2002) 282–289.
- [31] A. Hovestad, L.J.J. Janssen, Electrochemical codeposition of inert particles in a metallic matrix, *J. Appl. Electrochem.* 25 (1995) 519–527.
- [32] S.-C. Wang, W.-C.J. Wei, Kinetics of electroplating process of nano-sized ceramic particle/Ni composite, *Mater. Chem. Phys.* 78 (2001) 574–580.
- [33] S.-C. Wang, W.-C.J. Wei, Electrokinetic Properties of Nanosized SiC Particles in Highly Concentrated Electrolyte Solutions, *J. Am. Ceram. Soc.* 84 (2001) 1411–1414.

- [34] A. Bund, D. Thiemig, Influence of bath composition and pH on the electrocodeposition of alumina nanoparticles and nickel, *Surf. Coat. Technol.* 201 (2007) 7092–7099.
- [35] W.-B. Chu, J.-W. Yang, T.-J. Liu, C. Tiu, J. Guo, The effects of pH, molecular weight and degree of hydrolysis of poly(vinyl alcohol) on slot die coating of PVA suspensions of TiO₂ and SiO₂, *Colloids Surf., A* 302 (2007) 1–10.
- [36] M. Kenjiro, U. Takahisa, H. Tetsuya, E. Kunio, Effects of Surfactants and Surface Treatment on Aqueous Dispersion of Silicon Carbide, *Bull. Chem. Soc. Jpn.* 60 (1987) 89–94.
- [37] D. Aslanidis, The Electrolytic Codeposition of Silica and Titania Modified Silica with Zinc, *J. Electrochem. Soc.* 144 (1997) 2352.
- [38] T. Lampke, B. Wielage, D. Dietrich, A. Leopold, Details of crystalline growth in co-deposited electroplated nickel films with hard (nano)particles, *Appl. Surf. Sci.* 253 (2006) 2399–2408.
- [39] L. Stappers, J. Fransaer, Growth of Metal around Particles during Electrodeposition, *J. Electrochem. Soc.* 153 (2006) C472.
- [40] Y. Yao, S. Yao, L. Zhang, H. Wang, Electrodeposition and mechanical and corrosion resistance properties of Ni–W/SiC nanocomposite coatings, *Mater. Lett.* 61 (2007) 67–70.
- [41] A. Zoikis-Karathanasis, E.A. Pavlatou, N. Spyrellis, Pulse electrodeposition of Ni–P matrix composite coatings reinforced by SiC particles, *J. Alloys Compd.* 494 (2010) 396–403.
- [42] M. Stroumbouli, P. Gyftou, E.A. Pavlatou, N. Spyrellis, Codeposition of ultrafine WC particles in Ni matrix composite electrocoatings, *Surf. Coat. Technol.* 195 (2005) 325–332.
- [43] H.-K. Lee, H.-Y. Lee, J.-M. Jeon, Codeposition of micro- and nano-sized SiC particles in the nickel matrix composite coatings obtained by electroplating, *Surf. Coat. Technol.* 201 (2007) 4711–4717.
- [44] T.J. Mason, J.P. Lorimer, D.J. Walton, Sonoelectrochemistry, *Ultrason.* 28 (1990) 333–337.
- [45] C.E. Brennen, *Cavitation and bubble dynamics*, Oxford University Press, New York, Oxford, 1995.
- [46] I. Tudela, Y. Zhang, M. Pal, I. Kerr, A.J. Cobley, Ultrasound-assisted electrodeposition of composite coatings with particles, *Surf. Coat. Technol.* 259 (2014) 363–373.
- [47] C. Zanella, M. Lekka, S. Rossi, F. Deflorian, Study of the influence of sonication during the electrodeposition of nickel matrix nanocomposite coatings on the protective properties, *Corros. Rev.* 29 (2011) 253–260.
- [48] C. Zanella, M. Lekka, P.L. Bonora, Effect of ultrasound vibration during electrodeposition of Ni–SiC nanocomposite coatings, *Surf. Eng.* 26 (2013) 511–518.
- [49] D. Dietrich, I. Scharf, D. Nickel, L. Shi, T. Grund, T. Lampke, Ultrasound technique as a tool for high-rate incorporation of Al₂O₃ in NiCo layers, *J. Solid State Electrochem.* 15 (2011) 1041–1048.

- [50] E. García-Lecina, I. García-Urrutia, J.A. Díez, J. Morgiel, P. Indyka, A comparative study of the effect of mechanical and ultrasound agitation on the properties of electrodeposited Ni/Al₂O₃ nanocomposite coatings, *Surf. Coat. Technol.* 206 (2012) 2998–3005.
- [51] H.-Y. Zheng, M.-Z. An, Electrodeposition of Zn–Ni–Al₂O₃ nanocomposite coatings under ultrasound conditions, *J. Alloys Compd.* 459 (2008) 548–552.
- [52] E. García-Lecina, I. García-Urrutia, J.A. Díez, J. Fornell, E. Pellicer, J. Sort, Codeposition of inorganic fullerene-like WS₂ nanoparticles in an electrodeposited nickel matrix under the influence of ultrasonic agitation, *Electrochim. Acta* 114 (2013) 859–867.
- [53] B. Bakhit, A. Akbari, Effect of particle size and co-deposition technique on hardness and corrosion properties of Ni–Co/SiC composite coatings, *Surf. Coat. Technol.* 206 (2012) 4964–4975.
- [54] A. Góral, M. Nowak, K. Berent, B. Kania, Influence of current density on microstructure and properties of electrodeposited nickel-alumina composite coatings, *J. Alloys Compd.* 615 (2014) S406–S410.
- [55] S. Shawki, Z. Abdel Hamid, Deposition of high wear resistance of Ni-composite coatings, *Anti-Corrosion Method & Mater.* 44 (1997) 178–185.
- [56] P. Gyftou, E.A. Pavlatou, N. Spyrellis, Effect of pulse electrodeposition parameters on the properties of Ni/nano-SiC composites, *Appl. Surf. Sci.* 254 (2008) 5910–5916.
- [57] P. Gyftou, M. Stroumbouli, E.A. Pavlatou, N. Spyrellis, Electrodeposition of Ni/SiC Composites by Pulse Electrolysis, *Trans. IMF* 80 (2002) 88–91.
- [58] E.A. Pavlatou, M. Stroumbouli, P. Gyftou, N. Spyrellis, Hardening effect induced by incorporation of SiC particles in nickel electrodeposits, *J. Appl. Electrochem.* 36 (2006) 385–394.
- [59] E.J. Podlaha, Pulse-Reverse Plating of Nanocomposite Thin Films, *J. Electrochem. Soc.* 144 (1997) L200.
- [60] P. Xiong-Skiba, D. Engelhaupt, R. Hulguin, B. Ramsey, Effect of Pulse Plating Parameters on the Composition of Alumina/Nickel Composite, *J. Electrochem. Soc.* 152 (2005) C571.
- [61] C. Kollia, Z. Loizos, N. Spyrellis, Influence of pulse reversed current technique on the crystalline orientation and surface morphology of nickel electrodeposits, *Surf. Coat. Technol.* 45 (1991) 155–160.
- [62] E.J. Podlaha, Selective Electrodeposition of Nanoparticulates into Metal Matrices, *Nano Lett.* 1 (2001) 413–416.
- [63] M. Hashiba, H. Okamoto, Y. Nurishi, K. Hiramatsu, The zeta-potential measurement for concentrated aqueous suspension by improved electrophoretic mass transport apparatus -- application to Al₂O₃, ZrO₃ and SiC suspensions, *J Mater Sci* 23 (1988) 2893–2896.
- [64] M. Kaisheva, J. Fransaer, Influence of the Surface Properties of SiC Particles on Their Codeposition with Nickel, *J. Electrochem. Soc.* 151 (2004) C89.

- [65] F. Kılıç, H. Gül, S. Aslan, A. Alp, H. Akbulut, Effect of CTAB concentration in the electrolyte on the tribological properties of nanoparticle SiC reinforced Ni metal matrix composite (MMC) coatings produced by electrodeposition, *Colloids Surf., A* 419 (2013) 53–60.
- [66] S.M. Lari Baghal, A. Amadeh, M. Heydarzadeh Sohi, S.M.M. Hadavi, The effect of SDS surfactant on tensile properties of electrodeposited Ni-Co/SiC nanocomposites, *Mater. Sci. Eng., A* 559 (2013) 583–590.
- [67] S.H. Yeh, C.C. Wan, Codeposition of SiC powders with nickel in a Watts bath, *J. Appl. Electrochem.* 24 (1994) 993–1000.
- [68] A. Góral, Nanoscale structural defects in electrodeposited Ni/Al₂O₃ composite coatings, *Surf. Coat. Technol.* 319 (2017) 23–32.
- [69] M. Ortolani, C. Zanella, C.L. Azanza Ricardo, P. Scardi, Elastic grain interaction in electrodeposited nanocomposite Nickel matrix coatings, *Surf. Coat. Technol.* 206 (2012) 2499–2505.
- [70] A.J. Schwartz, M. Kumar, B.L. Adams, D.P. Field, *Electron Backscatter Diffraction in Materials Science*, Springer US, Boston, MA, 2009.
- [71] R.L. Smith, G.E. Sandly, An Accurate Method of Determining the Hardness of Metals, with Particular Reference to Those of a High Degree of Hardness, *Proceedings of the Institution of Mechanical Engineers* 102 (1922) 623–641.
- [72] R. Starosta, A. Zielinski, Effect of chemical composition on corrosion and wear behaviour of the composite Ni-Fe-Al₂O₃ coatings, *J. Mater. Process. Technol.* 157–158 (2004) 434–441.
- [73] T. Borkar, S.P. Harimkar, Effect of electrodeposition conditions and reinforcement content on microstructure and tribological properties of nickel composite coatings, *Surf. Coat. Technol.* 205 (2011) 4124–4134.
- [74] S. Spanou, E.A. Pavlatou, N. Spyrellis, Ni/nano-TiO₂ composite electrodeposits, *Electrochim. Acta* 54 (2009) 2547–2555.
- [75] S.K. Kim, H.J. Yoo, Formation of bilayer Ni-SiC composite coatings by electrodeposition, *Surf. Coat. Technol.* 108–109 (1998) 564–569.
- [76] R.P. Socha, P. Nowak, K. Laajalehto, J. Väyrynen, Particle-electrode surface interaction during nickel electrodeposition from suspensions containing SiC and SiO₂ particles, *Colloids Surf., A* 235 (2004) 45–55.
- [77] P. Nowak, R.P. Socha, M. Kaisheva, J. Franssaer, J.-P. Celis, Z. Stoinov, Electrochemical investigation of the codeposition of SiC and SiO₂ particles with nickel, *J. Appl. Electrochem.* 30 (2000) 429–437.
- [78] H. Ohshima, *Electrical phenomena at interfaces and biointerfaces: Fundamentals and applications in nano-, bio-, and environmental sciences*, John Wiley & Sons, 2012.
- [79] I. Tudela, Y. Zhang, M. Pal, I. Kerr, A.J. Cobley, Ultrasound-assisted electrodeposition of thin nickel-based composite coatings with lubricant particles, *Surf. Coat. Technol.* 276 (2015) 89–105.

- [80] M. Aroyo, N. Tzonev, Pulse periodic reverse plating: New possibilities for electrodeposition of metal coatings with improved properties: Part 1, Plating and surface finishing 89 (2002) 48–53.
- [81] M.-D. Ger, Electrochemical deposition of nickel/SiC composites in the presence of surfactants, Mater. Chem. Phys. 87 (2004) 67–74.
- [82] I. Tudela, Y. Zhang, M. Pal, I. Kerr, T.J. Mason, A.J. Cobley, Ultrasound-assisted electrodeposition of nickel, Surf. Coat. Technol. 264 (2015) 49–59.

APPENDED PAPERS

Supplement I

S. Pinate, F. Eriksson, P. Leisner, C. Zanella; Effects of particles codeposition and ultrasound agitation on the electrocrystallisation of Ni nanocomposites.

Manuscript. Submitted for journal publication.

Supplement II

S. Pinate, A. Ispas, P. Leisner, A. Bund, C. Zanella; Electrocodeposition of Ni composites and surface modification of SiC nanoparticles.

Manuscript.

Supplement III

S. Pinate, P. Leisner, C. Zanella; Codeposition of nano-SiC particles by pulse-reverse electroplating.

Manuscript.